2019

THE ROLE OF NRF2 SIGNALLING IN CELL PROLIFERATION AND TUMORIGENESIS OF CHROMIUM TRANSFORMED HUMAN BRONCHIAL EPITHELIAL CELLS

Marco Antonio de Freitas Clementino
University of Kentucky, marco.clementino22@gmail.com
Author ORCID Identifier:
 https://orcid.org/0000-0002-0628-8047
Digital Object Identifier: https://doi.org/10.13023/etd.2019.047

STUDENT AGREEMENT:

I represent that my thesis or dissertation and abstract are my original work. Proper attribution has been given to all outside sources. I understand that I am solely responsible for obtaining any needed copyright permissions. I have obtained needed written permission statement(s) from the owner(s) of each third-party copyrighted matter to be included in my work, allowing electronic distribution (if such use is not permitted by the fair use doctrine) which will be submitted to UKnowledge as Additional File.

I hereby grant to The University of Kentucky and its agents the irrevocable, non-exclusive, and royalty-free license to archive and make accessible my work in whole or in part in all forms of media, now or hereafter known. I agree that the document mentioned above may be made available immediately for worldwide access unless an embargo applies.

I retain all other ownership rights to the copyright of my work. I also retain the right to use in future works (such as articles or books) all or part of my work. I understand that I am free to register the copyright to my work.

REVIEW, APPROVAL AND ACCEPTANCE

The document mentioned above has been reviewed and accepted by the student's advisor, on behalf of the advisory committee, and by the Director of Graduate Studies (DGS), on behalf of the program; we verify that this is the final, approved version of the student's thesis including all changes required by the advisory committee. The undersigned agree to abide by the statements above.

Marco Antonio de Freitas Clementino, Student

Dr. Zhuo Zhang, Major Professor

Dr. Isabel Mellon, Director of Graduate Studies

THE ROLE OF NRF2 SIGNALLING IN CELL PROLIFERATION AND
TUMORIGENESIS OF CHROMIUM TRANSFORMED HUMAN BRONCHIAL
EPITHELIAL CELLS

_____

DISSERTATION
_____

A dissertation submitted in partial fulfillment of the
requirements for the degree of Doctor of Philosophy in the
College of Medicine at the University of Kentucky

By
Marco Antonio de Freitas Clementino
Lexington, Kentucky
Director: Dr. Zhuo Zhang, Professor of Toxicology and Cancer Biology
Lexington, Kentucky
2019

ABSTRACT OF DISSERTATION

THE ROLE OF NRF2 SIGNALLING IN CELL PROLIFERATION AND
TUMORIGENESIS OF CHROMIUM TRANSFORMED HUMAN BRONCHIAL
EPITHELIAL CELLS

Hexavalent Chromium (Cr(VI) induces malignant cell transformation in normal bronchial epithelial (BEAS-2B) cells. Cr(VI)-transformed cells exhibit increased level of antioxidants, are resistant to apoptosis, and are tumorigenic. RNAseq analysis in Cr(VI)-transformed cells showed that expression of transcripts associated with mitochondrial oxidative phosphorylation is reduced, and the expression of transcripts associated with pentose phosphate pathway, glycolysis, and glutaminolysis are increased. Sirtuin-3 (SIRT3) regulates mitochondrial adaptive response to stress, such as metabolic reprogramming and antioxidant defense mechanisms. SIRT3 was upregulated and it positively regulated mitochondrial oxidative phosphorylation in Cr(VI)-transformed cells. Our results suggests that SIRT3 plays an important role in mitophagy deficiency of Cr(VI)-transformed cells. Furthermore, SIRT3 knockdown suppressed cell proliferation and tumorigenesis of Cr(VI)-transformed cells. Nrf2 is a transcription factor that regulates oxidative stress response. This study investigated the role of Nrf2 in regulating metabolic reprogramming in Cr(VI)-transformed cells. We observed that in Cr(VI)-transformed cells p-AMPK^{thr172} was increased, when compared to normal BEAS-2B cells. Additionally, Nrf2 knockdown reduced p-AMPK^{thr172}. Our results suggest that Nrf2 regulated glycolytic shift via AMPK regulation of PFK1/PFK2 pathway. Furthermore, our results showed that Nrf2 constitutive activation in Cr(VI-transformed cells increased cell proliferation and tumorigenesis. Overall this dissertation demonstrated that Cr(VI)-transformed cells undergo metabolic reprogramming. We demonstrated that Nrf2 constitutive activation plays decisive role on metabolic reprogramming induction, and SIRT3 activation contributing to increased cancer cell proliferation and tumorigenesis.

Marco Clementino
Marco Antonio de Freitas Clementino

March 8th, 2019
Date

THE ROLE OF NRF2 SIGNALLING IN CELL PROLIFERATION AND
TUMORIGENESIS OF CHROMIUM TRANSFORMED HUMAN BRONCHIAL
EPITHELIAL CELLS

By
Marco Clementino

Dr. Zhuo Zhang
Director of Dissertation

Dr. Isabel Mellon
Director of Graduate Studies

March 8th, 2019
Date

TABLE OF CONTENTS

LIST OF TABLES

LIST OF FIGURES

CHAPTER 1. Oxidative stress and metabolic reprogramming in Cr(VI) carcinogenesis

1.1 Abstract

Cr(VI)-containing compounds are well-established lung carcinogens. Chronic exposure of human bronchial epithelial cells (BEAS-2B) to Cr(VI) is able to induce malignant cell transformation, the first stage of metal carcinogenesis. These Cr(VI)-transformed cells exhibit increased levels of antioxidants, reduced capacity of generating reactive oxygen species (ROS), and increased apoptosis resistance, which together promote tumorigenesis of Cr(VI)-transformed cells, the second stage of Cr(VI)-carcinogenesis. The mechanism of Cr(VI)-induced carcinogenesis is still under investigation. Recent studies indicated that increased ROS generation causes malignant cell transformation, the first stage of Cr(VI) carcinogenesis. Reduced ROS generation causes development of apoptosis resistance of Cr(VI)-transformed cells, the second stage of Cr(VI)-carcinogenesis. Malignant transformed cells adapt metabolism to support tumor initiation and progression. Altered metabolic activities directly participate in the process of cell transformation or support a large requirement for nucleotides, amino acids, and lipids for tumor growth. In Cr(VI)-transformed cells, mitochondrial oxidative phosphorylation is defective, and pentose phosphate pathway, glycolysis, and glutaminolysis are upregulated. These metabolic reprogramming supports rapid cell proliferation and contributes to tumorigenesis of Cr(VI)-transformed cells. This chapter summarizes the current progress in the studies of metabolic reprogramming and Cr(VI) carcinogenesis with emphasis on the metabolic enzymes and oxidative stress related major oncogenic pathways.

1.2 Introduction

When normal cells are converted to malignantly transformed cells and progress to cancer, their metabolism is altered. In contrast to the normal

differentiated cells which rely mainly on mitochondrial oxidative phosphorylation (OXPHOS) for generation of needed energy, cancer cells depend on anaerobic glycolysis, a phenomenon called "the Warburg effect" for energy. This altered cellular metabolism, also called metabolic reprogramming, is recognized as one of the cancer phenotypes. Accumulative evidence reveals that various oncogenic pathways are involved in the metabolic regulation. Expression of glucose transporters and glycolytic enzymes are increased in numerous cancers and may contribute to tumor progression (Majumder et al. 2004; Shackelford et al. 2009). It has been reported that oncogenes and tumor suppressor genes, such as hypoxia inducible factor 1 (HIF-1) (Stohs et al. 2000), c-Myc (Wang et al. 2011; Yao et al. 2008; Ye et al. 1995), p53 (Barchowsky et al. 1999; Liu et al. 2001), and PI3K/Akt (Harris and Shi 2003), directly promote metabolism of glucose and glutamine.

Chromate (Cr(VI)) compounds, widely used in industry, have been shown to be toxic and carcinogenic on humans (Langard 1990; 1993; Machle and Gregorius 1948; Wilbur et al. 2012). Cr(VI) is structurally similar to sulfate and phosphate anions; therefore, it readily enters into the cells via non-specific anion transporters (Zhitkovich 2011). Once inside the cells, Cr(VI) undergoes a series of metabolic reductions and forms intermediate Cr species, including Cr(V) and Cr(IV), and is finally reduced to Cr(III) (Zhitkovich 2005; 2011). In the Cr(VI) reduction process, reactive oxygen species (ROS) are produced, resulting in oxidative DNA damage. The intermediates Cr(V) and Cr(IV) and the final product Cr(III) are very reactive, causing Cr-DNA adducts and genomic alterations. Epidemiological studies have shown that occupational exposure to Cr(VI) is associated with a high rate of lung cancer in workers employed in these industries (Langard 1990; 1993; Machle and Gregorius 1948; Wilbur et al. 2012). Environmental Cr(VI) exposure is also a public health concern and is associated with long-term carcinogenic effects of the lung (Langard 1993; Woodruff et al. 1998). Though the mechanisms of Cr(VI) carcinogenesis have not yet been fully understood, is generally believed that ROS are important in inducing malignant cell transformation, the first stage of metal carcinogenesis (Shi and Dalal 1989;

Wang et al. 2011; Yao et al. 2008; Ye et al. 1995). ROS can be involved in various carcinogenic processes (Shi and Dalal 1989). Recent studies from our laboratory has shown that once cells are malignantly transformed, the capacity of those transformed cells to generate ROS is sharply reduced, leading to the development of apoptosis resistant and subsequent tumorigenesis (Zhang et al. 2015b). Thus, the decreased ROS generation in Cr(VI)-transformed cells is oncogenic in promoting tumorigenesis, the second stage of metal carcinogenesis. The oncogenic role of ROS in the first stage of Cr(VI) carcinogenesis (malignant cell transformation) and anti-oncogenic role in the second stage (tumorigenesis) reflects the metabolic reprogramming during the change from normal cells to malignantly transformed cells. Although this reprogramming may play an important role in the mechanism of metal carcinogenesis in general and Cr(VI) carcinogenesis in particular, its underlying mechanism remains to be investigated. This chapter provides an outline on progress and future perspectives in oxidative stress and metabolic reprogramming in Cr(VI) carcinogenesis.

1.3   Glycolysis

Glucose homeostasis is controlled by glycolysis/oxidative phosphorylation (OXPHOS) and gluconeogenesis pathway. Glycolysis is the enzymatic conversion of glucose into lactate, which produces 2 ATP per glucose molecule. In the presence of oxygen, normal cells primarily adopt mitochondrial OXPHOS to produce 36 ATP per glucose molecule. Cancer cells favor aerobic glycolysis over OXPHOS to meet their energy demand, suggesting that cancer cells are adapted to survive and proliferate in the absence of mitochondrial ATP production. The mitochondria play a major role in supplying energy and regulating ROS. Although various mechanisms of carcinogenesis induced by Cr(VI) have been demonstrated, it is generally believed that Cr(VI)-induced oxidative stress is important in converting normal cells to malignantly transformed cells. It has been reported that Cr(VI) suppressed all five mitochondrial complexes involved in OXPHOS in a variety of model systems with more potency

3

of complexes I, II, and V than complexes III and IV. Our study showed that in Cr(VI)-transformed cells, mitochondrial ATP production was reduced and non-mitochondrial oxygen consumption was increased, indicating a defect in mitochondrial ATP production (Dai et al. 2017). The results from RNA sequencing analysis showed in Cr(VI)-transformed cells compared to passage matched cells, the levels of various enzymes involved in all five complexes was reduced (Table 2), demonstrating that Cr(VI)-transformed cells are defective in mitochondrial ATP generation.

Aerobic glycolysis, maximizing ATP production, does not require an increase in mitochondrial capacity (Fan et al. 2013). Cr(VI)-transformed cells generated more lactate without significant changes in glucose uptake and ATP production, indicating a switch from mitochondrial respiration to glycolysis (Dai et al. 2017). The results from Table 1 show that several glycolysis enzymes including ADP-specific glucokinase (ADPGK), enolase 1 (ENO1), hexokinase (HK2), phosphoglycerate kinase (PGK1), dihydrolipoamide S-acetyltransferase (DLAT), pyruvate dehydrogenase E1 (PDHA1), glucose-6-phosphatase 3 (G6PC3), pyruvate kinase (PKM), aldolase A (ALDOA), phosphofructokinase (PFKM) were upregulated in Cr(VI)-transformed cells, indicating that Cr(VI)-transformed cells utilize glycolysis for energy for survival under defective mitochondrial function. It should be noted that many metabolic enzymes are regulated through allostery and/or post-translation. For example, pyruvate dehydrogenase, a complex with multiple subunits and cofactors, whose activity is regulated by phosphorylation/dephosphorylation. Thus characterization of metabolic flux together with transcriptomics is a more appropriate way to evaluate the metabolic changes upon Cr(VI) exposure. Cancer stem cells (CSCs) or cancer-initiating cells, a small subset of malignant cells that exhibit high capacity of self-renewal and differentiation, have been reported to utilize aerobic glycolysis for biosynthesis and energy requirement (Dong et al. 2013). About 1% of Cr(VI)-transformed cells have been identified as CSCs and these CSCs are metabolically inactive as evidenced by dramatic reductions of glucose uptake, lactate production, and ATP content (Dai et al. 2017). These small population of

4

CSCs may be the driving force for the increased glycolysis of Cr(VI)-transformed cells.

Energy metabolism is a balanced mechanism controlled by catabolic (glycolysis and oxidative phosphorylation) and anabolic (gluconeogenesis) reactions. Fructose-1, 6-bisphosphatase (FBP1), a rate limiting enzyme in gluconeogenesis, catalyzes the hydrolysis of fructose-1, 6-bisphosphate to fructose 6-phosphate and inorganic phosphate. It has been reported that loss of FBP1 is correlated with advanced stage and poor prognosis of cancer (Chen et al. 2011; Zhang et al. 2016a). Inhibition of FBP1 increased glucose uptake and lactate secretion in HK-2 human renal cells and in consistent, forced expression of FBP1 reduced glucose uptake, lactate secretion, and glucose-derived TCA cycle intermediates in renal carcinoma RCC10 cells (Li et al. 2014). In CSCs low level of FBP1 is beneficial due to (a) induction of glycolysis and increased glucose uptake, facilitating the production of glycolysis intermediates and the energy supply during hypoxia and (b) inhibition of ROS generation induced by mitochondrial complex 1, protecting cells from oxidative stress (Dong et al. 2017). In Cr(VI)-transformed cells FBP1 level is low compared to that in passage-matched normal cells and FBP1 is lost in CSCs (Dai et al. 2017). Ectopic expression of FBP1 in CSCs reduced glucose uptake, lactate production, and glycolysis (Dai et al. 2017), indicating that FBP1 plays an important role in glucose metabolism.

HIF-1α is important in angiogenesis and in cancer development (Dong et al. 2017; Maxwell et al. 1997; Ryan et al. 1998; Vaupel 2004). Its level is elevated in more than half of human cancers and their metastases (Birner et al. 2000; Blancher et al. 2000; Giatromanolaki et al. 2001; Huss et al. 2001; Kallio et al. 1999; Zhong et al. 1999). The occurrence of Warburg effect indicates the activation of oncogenic signaling, such as hypoxia inducible factor (HIF)-1α, resulting in promotion of glucose uptake and anabolic metabolism (Fan et al. 2013). This transcription factor upregulates many glycolytic enzymes, in which their gene promoters contain consensus binding motif 5'-(C/G/T)ACGTGC(G/T)-

3' of HIF-1α. HIF-1α protein is rapidly degraded at normoxia via pVHL-mediated ubiquitin-proteasome pathway, whereas hypoxia blocks degradation of HIF-1α protein, leading to its accumulation (Huang et al. 1996). Stabilization of HIF-1α modulates metabolic adaptation to low molecular oxygen levels through increase of cellular glycolysis (Bertout et al. 2008). HIF-1α upregulates glucose transporters and glycolytic enzymes (Semenza 2010). HIF1α also upregulates pyruvate dehydrogenase kinases (PDKs), the enzymes control entry of glucose-derived pyruvate into tricarboxylic acid (TCA) cycle (Kim et al. 2006; Papandreou et al. 2006). HIF-1α was activated in Cr(VI)-repeatedly exposed cells (Kim et al. 2016) or in Cr(VI)-transformed cells (Kaczmarek et al. 2007). HIF-1α is able to bind to five glycolytic enzymes including phosphofructokinase (PFK), aldolase (ALDA), phosphoglycerate kinase 1 (PGK1), enolase 1 (ENO1), pyruvate kinase (PKM), and lactate dehydrogenase (LDHA) (Dang et al. 2008). The results from Table 1 show that these five enzymes were upregulated in Cr(VI)-transformed cells. It is very likely that HIF-1α directly binds to the promoters of these glycolytic enzymes. FBP1 binds to HIF-1α inhibitory domain, blocking its induction of glycolysis (Li et al. 2014). Thus, reduced FBP1 level in Cr(VI)-transformed cells may induce glycolysis through decreased binding to HIF1α.

Phosphorylation on metabolic enzymes also contributes to aerobic glycolysis (Bensinger and Christofk 2012). PI3K/Akt phosphorylates hexokinase and PFK-2 (Elstrom et al. 2004) and promotes GLUT expression and plasma membrane localization (Robey and Hay 2009), suggesting that activation of PI3K/Akt pathway promotes the Warburg effect by stimulating glucose uptake and further catabolism by glycolysis. It has been demonstrated that PI3K/Akt/p38 MAPK is responsible for HIF-1α activation in Cr(VI)-transformed cells (Kim et al. 2016), indicating involvement of PI3K/Akt/p38 in the upregulation of glycolysis of Cr(VI)-transformed cells.

1.4 Pentose phosphate pathway (PPP)

Pentose phosphate pathway (PPP), a classic metabolic pathway, consists of oxidative and non-oxidative branches. The oxidative PPP converts glucose-6-phosphate (G6P), a glycolytic intermediate, into ribulose-5-phosphate and generates NADPH, which is used for glutathione production, detoxification, and biosynthesis of lipids. The non-oxidative branch involves reversible carbon-exchanging reactions with the final products as fructose-6-phosphate and glyceraldehyde-3-phosphate, which participate in glycolysis and downstream metabolic pathways (Riganti et al. 2012). PPP is upregulated in many types of tumors (Deberardinis et al. 2008; Riganti et al. 2012). The activities of glucose-6-phosphate dehydrogenase (G6PD) and transketolase (TKT), key PPP enzymes, were increased in cancer cells (Hartmannsberger et al. 2011; Jonas et al. 1992). An early study indicated that short-term exposure of human erythrocytes to Cr(VI) did not exhibit effect on any of the three PPP enzymes, glucose-6-phosphate dehydrogenase (G6PDH), 6-phosphogluconate dehydrogenase (PGD), or transsketolase (TKT) (Koutras et al. 1964). Our transcriptomic analysis show that in Cr(VI)-transformed cells expressions of several PPP enzymes including phosphorybosyl pyrophosphate synthase 1 & 2 (PRPS1/2), G6PD, ribulose 5-phosphate 3-epimerase (RPE), transaldolase (TALDO1), PGD, ribose 5-phosphate isomerase (RPIA), aldolase A (ALDOA), and TKT were elevated compared to passage-matched normal cells (Table 1).

Nuclear factor (erythroid-derived 2)-like 2 (Nrf2) is a key transcription factor that regulates antioxidant proteins to neutralize ROS and to restore cellular redox balance (Chan et al. 2001; Kobayashi and Yamamoto 2006). This transcription factor plays dual roles in carcinogenesis. Activation of inducible Nrf2 decreases malignant cell transformation carcinogenesis via decrease of oxidative stress (Hayes et al. 2010; Hu et al. 2010; Sporn and Liby 2012). Conversely, constitutively activated Nrf2 exerts oncogenic effects by protecting cancer cells from oxidative stress and chemotherapeutics (Kansanen et al. 2013b; Wang et al. 2008). Constitutive activation of Nrf2 has been identified in several types of

7

human cancer cell lines and tumors (Lau et al. 2013; Ohta et al. 2008; Sporn and Liby 2012; Tong et al. 2006). Cancers with high Nrf2 level are associated with poor prognosis (Shibata et al. 2008; Solis et al. 2010), resistance to therapeutics, and rapid proliferation (Singh et al. 2008; Zhang et al. 2010). In addition to its role in regulation of oxidative stress, Nrf2 is also involved in the anabolic metabolism (Mitsuishi et al. 2012; Singh et al. 2008). Nrf2 directly activates six genes involved in the PPP and nicotinamide adenine dinucleotide phosphate (NADPH) production pathway, including G6PD, PGD, TKT, TALDO1, and malicenzyme1 (ME1), through binding of Nrf2 to antioxidant response elements (AREs) of these gene promoters (Mitsuishi et al. 2012). Using [U-^{13}C$_6$] tracer assay, it has been demonstrated that Nrf2 is required for purine nucleotide synthesis (Mitsuishi et al. 2012). During metabolic reprogramming Nrf2 redirects glucose and glutamine into anabolic pathways, protecting cancer cells from oxidative damage (Mitsuishi et al. 2012). Activation of Nrf2 increases glucose uptake through the PPP, subsequently producing NADPH (Hawkins et al. 2016; Heiss et al. 2013; Mitsuishi et al. 2012). Our studies have showed that Nrf2 is constitutively activated in Cr(VI)-transformed cells and inhibition of Nrf2 suppresses tumorigenesis of Cr(VI)-transformed cells . Whether Nrf2 regulates PPP remains to be investigated in Cr(VI)-transformed cells, our preliminary results indicate that Nrf2 positively regulates G6PD, PGD, TKT, and TALDO1, resulting in upregulation of PPP.

1.5 Glutaminolysis

Along with increased aerobic glycolysis, increased glutaminolysis is recognized as a key feature of the metabolic profile of cancer cells (Daye and Wellen 2012). In addition to glycolysis, many tumors also depend on glutaminolysis to fuel their cellular bioenergetics and metabolism. Glutaminolysis catabolizes glutamine to downstream metabolites such as glutamate and α-ketoglutarate, important intermediates to fuel TCA cycle of tumors. Similar to glycolysis, glutaminolysis supplies cancer cells with both ATP and crucial precursors for continuous biosynthesis and accelerated proliferation (Dang 2010;

DeBerardinis and Cheng 2010). Table 1 shows that levels of three glutaminolytic enzymes including glutaminase (GLS), aspartate aminotransferase 2 (GOT2), and glutamine fructose-6-phosphate transaminase 1 (GFPT1) were elevated in Cr(VI)-transformed cells, suggesting upregulation of glutaminolysis.

Nrf2 increases glutamine consumption through enhancing glutaminolysis and glutathione synthesis. Nrf2 indirectly activates transcription factor 4 (ATF4), which regulates serine/glycine biosynthesis enzymes, supplying the substrates for glutathione and nucleotide production (DeNicola et al. 2015). Nrf2 promotes glutathione synthesis from glutamine (Mitsuishi et al. 2012). Nrf2 induces glutamate cysteine ligase (GCL), a key enzyme for glutathione synthesis, by directly activating the GCL encoding genes (Sekhar et al. 2003). Nrf2 also increases the supply of cysteine by direct activation of the gene encoding cysteine transporter SLC7A11 (Sasaki et al. 2002). Nrf2 is constitutively activated in Cr(VI)-transformed cells, the mechanism of Nrf2 in regulation of glutaminolysis in Cr(VI)-transformed cells has not yet been reported. In consideration the findings from Table 1, it is very possible that Nrf2 targets GLS, which metabolizes glutamine to glutamate, providing a key nitrogen donor and carbon supply for the TCA cycle of Cr(VI)-transformed cells.

1.6   Conclusions

Metabolic reprogramming, a major hallmark of cancer, is characterized by upregulations of glycolysis, glutaminolysis, lipid metabolism and pentose phosphate pathway. The metabolic program provides energy and metabolites to support rapid growth and proliferation of cancer cells. Chronic exposure of the cells to Cr(VI) causes malignant transformation. Similar to other cancer cells, these Cr(VI)-transformed cells have increased need for nutrients, energy, and biosynthetic activities to produce all macromolecular components during each passage through cell cycle. Cr(VI)-induced tumorigenesis is a chronic process. Among all studies related to bioenergetic phenotype induced by Cr(VI), most of studies focused on the short-term exposure, only a few studies investigated the

metabolic activities after long-term exposure to Cr(VI). For several decades, there has been a concentrated effort to identify the mechanisms of Cr(VI) carcinogenesis. However, little has been done to determine how changes of genes involved in glucose and glutamine metabolism contribute to Cr(VI) carcinogenesis. Cr(VI) exposure interferes with metabolic transduction pathways through different levels, including gene expression, intracellular protein levels, and protein function. We speculate that oxidative stress plays an important role in these processes. Chronic exposure of the cells to Cr(VI) causes ROS generation, leading to malignant cell transformation. Cr(VI)-transformed cells exhibit reduced capacity to generate ROS and elevated levels of antioxidant enzymes, leading to development of apoptosis resistance. In Cr(VI)-transformed cells, constitutive activation of Nrf2 enhances the PPP and NADPH generation, promoting cell proliferation. A representative scheme of possible mechanisms of metabolic reprogramming in Cr(VI) carcinogenesis is summarized in Figure 1.

Table 1.1 Relative level of metabolic enzymes in Cr(VI)-transformed cells and passage matched normal cells

Gene Symbol	Target pathway	BEAS-2B	BEAS-2B-Cr(VI)
ADPGK	Glycolysis	0.4 ± 0.5	6.7 ± 3.2 *
ALDOA	Glycolysis/PPP	6.8 ± 4.3	254.9 ± 57.0 *
DLAT	Glycolysis	14.7 ± 1.0	21.6 ± 2.6 *
ENO1	Glycolysis	1.5 ± 0.6	71.6 ± 0.9 *
G6PC3	Glycolysis	50.7 ± 3.4	97.3 ± 14.9 *
GPI	Glycolysis	19.1 ± 4.0	73.8 ± 8.9 *
HK2	Glycolysis	21.2 ± 3.8	32.1 ± 2.8 *
PDHA1	Glycolysis	48.9 ± 4.5	158.5 ± 11.7 *
PFKM	Glycolysis	29.5 ± 4.7	83.9 ± 3.6 *
PGK1	Glycolysis	107.5 ± 36.4	221.7 ± 68.5
PKM	Glycolysis	112.5 ± 70.6	261 ± 73.9
G6PD	PPP	29.2 ± 5.3	142.3 ± 50.2 *
PGD	PPP	6.8 ± 3.1	31.4 ± 5.9 *
PRPS1	PPP	59.4 ± 1.9	135.2 ± 8.1 *
PRPS2	PPP	27.2 ± 0.1	53.6 ± 5.9 *
RPE	PPP	28.1 ± 1.7	39.0 ± 4.7 *
RPIA	PPP	20.1 ± 2.5	324.3 ± 85.5 *
TALDO1	PPP	28.8 ± 6.6	55.8 ± 7.7 *
TKT	PPP	151.9 ± 32.4	324.3 ± 85.5 *
GFPT1	Glutaminolysis	14.4 ± 1.4	26.8 ± 6.7 *
GLS	Glutaminolysis	19.3 ± 3.7	30.3 ± 10.4 *

Table 1.1 **Relative level of metabolic enzymes involved in glycolysis, PPP, and glutaminolysis**. Normal BEAS-2B cells (BEAS-2B) and Cr(VI)-transformed cells (BEAS-

2B-Cr) were subjected for extraction and purification of RNA using RNAeasy mini kit. Whole transcriptome sequencing analysis was performed using HiSeq 2500 Rapid Run. Differentially expressed genes involved in glycolysis, PPP, and glutaminolysis were detected using EBseq. A false detection rate analysis with 0.05 threshold was performed and considered as biostatistics difference (*, $p < 0.05$). Data represent mean ± SD (n=3).

Table 1.2 Relative level of enzymes involved in oxidative phosphorylation in Cr(VI)-transformed cells and passage-matched normal cells

Gene Symbol	Mitochondrial complex	BEAS-2B	BEAS-2B-Cr(VI)
NDUFA13	Complex I	58.1 ± 5.1	34.9 ± 12.2 *
NDUFA11	Complex I	10.0 ± 0.2	6.4 ± 1.0 *
NDUFC2	Complex I	154.6 ± 8.8	81.3 ± 23.5 *
NDUFS8	Complex I	182.5 ± 2.0	99.2 ± 26.7 *
NDUFS7	Complex I	71.7 ± 3.1	46.4 ± 13.4 *
NDUFS5	Complex I	544.2 ± 63.1	271.8 ± 21.4 *
NDUFB7	Complex I	254.3 ± 16.4	153.6 ± 29.6 *
NDUFV1	Complex I	12.5 ± 3.2	5.8 ± 1.2 *
NDUFA6	Complex I	105.5 ± 2.8	0.5 ± 0.8 *
NDUFA2	Complex I	152.4 ± 21.6	72.6 ± 20.1 *
SDHA	Complex II	246.5 ± 37.5	105.6 ± 20.1 *
UQCRC1	Complex III	108.1 ± 6.8	84.5 ± 18.0
UQCR11	Complex III	160.3 ± 15.1	101.5 ± 4.1 *
UQCR10	Complex III	103.6 ± 9.3	61.4 ± 9.1 *
UQCRH	Complex III	42.0 ± 3.1	26.0 ± 2.1 *
COX4I1	Complex IV	8.3 ± 1.2	3.4 ± 1.3 *
COX6A1	Complex IV	1.4 ± 0.5	0.7 ± 0.1 *
COX6B1	Complex IV	4.7 ± 1.1	1.8 ± 0.7 *
ATP5H	Complex V	631.8 ± 32.6	362.8 ± 11.1 *
ATP5L	Complex V	119.5 ± 9.5	87.3 ± 19.9 *
ATP5C1	Complex V	76.2 ± 15.7	1.6 ± 0.6 *

Table 1.2 **Relative level of enzymes involved in mitochondrial oxidative phosphorylation**. The method used is the same as that in Table 1. Genes involved in mitochondrial oxidative phosphorylation were detected using EBseq. A false detection

rate analysis with 0.05 threshold was performed and considered as biostatistics difference (*, $p < 0.05$). Data represent mean ± SD (n=3).
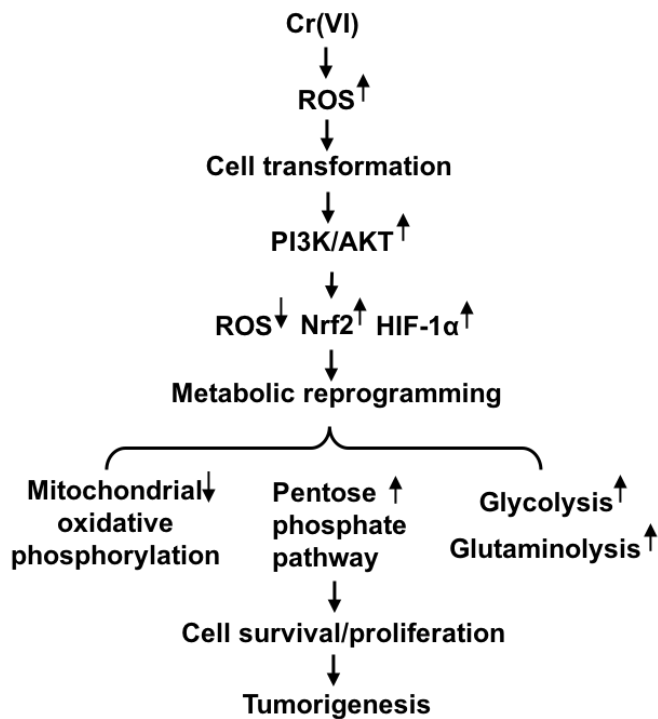
Figure 1.1 **Representative scheme of metabolic reprogramming in Cr(VI) carcinogenesis**. Chronic exposure of cells to Cr(VI) causes ROS generation which is responsible for malignant cell transformation. Once the cells are malignant transformed, those cells exhibit activated PI3K/Akt, reduced ROS generation, elevated antioxidant expressions and HIF-1α, resulting in reduction of mitochondrial oxidative phosphorylation and upregulations of pentose phosphate pathway, glycolysis and glutaminolysis, leading to tumorigenesis.

CHAPTER 2. CONSTITUTIVE ACTIVATION OF NAD-DEPENDENT SIRTUIN 3 PLAYS AN
IMPORTANT ROLE IN TUMORIGENESIS OF CHROMIUM(VI)-TRANSFORMED CELLS

2.1   Abstract

Chronic exposure of human bronchial epithelial BEAS-2B cells to
hexavalent chromium (Cr(VI)) causes malignant cell transformation. NAD-
dependent Sirtuin-3 (SIRT3) regulates mitochondrial adaptive response to stress,
such as metabolic reprogramming and antioxidant defense mechanisms. In
Cr(VI)-transformed cells, SIRT3 was upregulated and mitochondrial ATP
production and proton leak were reduced. Inhibition of SIRT3 by its shRNA
further decreased mitochondrial ATP production, proton leak and mitochondrial
mass and induced mitochondrial membrane depolarization, indicating that SIRT3
positively regulates mitochondrial oxidative phosphorylation and maintenance of
mitochondrial integrity. Mitophagy is critical to maintain proper cellular functions.
In Cr(VI)-transformed cells expressions of Pink 1 and Parkin, two mitophagy
proteins, were elevated, mitophagy remained similar as that in passage-matched
normal BEAS-2B cells, indicating that Cr(VI)-transformed cells are mitophagy
deficient. Knockdown of SIRT3 induced mitophagy, suggesting that SIRT3 plays
an important role in mitophagy deficiency of Cr(VI)-transformed cells. In Cr(VI)-
transformed cells, nuclear factor-(erythroid-derived 2)-like 2 (Nrf2) was
constitutively activated, and protein levels of p62 and p-p62^{Ser349} were elevated.
Inhibition of SIRT3 or treatment with carbonyl cyanide m-chloro phenyl hydrazine
(cccp) decreased the binding of p-p62^{Ser349} to Keap1, resulting in increased
binding of Keap1 to Nrf2 and consequently reduced Nrf2 activation. The results
from CHIP assay showed that in Cr(VI)-transformed cells binding of Nrf2 to
antioxidant response element (ARE) of SIRT3 gene promoter was dramatically
increased. Inhibition of SIRT3 suppressed cell proliferation and tumorigenesis of
Cr(VI)-transformed cells. Forced expression of SIRT3 in normal BEAS-2B cells
exhibited mitophagy deficient phenotype and increases in cell proliferation and
tumorigenesis. The present study demonstrated that upregulation of SIRT3

causes mitophagy deficiency, playing an important role in cell survival and tumorigenesis of Cr(VI)-transformed cells.

2.2   Introduction

Hexavalent chromium (Cr(VI)) has been classified as Group 1 human carcinogen by the International Agency for Research in Cancer (IARC). Environmental exposure to Cr(VI) has increased in the past decades due to usage of this metal in industry, agriculture, and technology endeavors (He et al. 2005; Shallari et al. 1998; Tchounwou et al. 2012). Our previous study showed that chronic exposure of bronchial epithelial (BEAS-2B) cells to Cr(VI) caused malignant cell transformation (Kim et al. 2015a). These transformed cells exhibited reduced capacity of generating ROS, development of apoptosis resistance, and increased angiogenesis, leading to cell survival and tumorigenesis (Kim et al. 2015a; Kim et al. 2016; Pratheeshkumar et al. 2016; Wang et al. 2011).

Mitochondria regulate energy homeostasis and cell death. Mitophagy, a selective form of autophagy for elimination of damaged mitochondria, is essential for the reduction of insufficient supply of ATP and excessive production of ROS. Defective mitophagy contributes to various diseases, including cancer (Bernardini et al. 2017; Chourasia et al. 2015; Kulikov et al. 2017). Mitophagy is regulated by two key mediators, the E3 ubiquitin ligase (Parkin, encoded by Park2 gene) and the Pten-induced putative kinase 1 (Pink1) (Durcan and Fon 2015; Eiyama and Okamoto 2015; Wei et al. 2015). Depolarization of mitochondrial membrane potential (MMP) causes translocation of Pink1 to the outer membrane, where it phosphorylates Parkin. Phosphorylated Parkin then ubiquitinates outer mitochondrial membrane proteins, targeting the organelle to undergo lysosomal autophagical degradation (Wei et al. 2015).

SIRT3, a major mitochondrial deacetylation enzyme, regulates metabolic homeostasis via mitochondria protein deacetylation (Finley and Haigis 2012; Giralt and Villarroya 2012). It was reported that SIRT3-deficient mice are below basal metabolic condition concomitant with increased mitochondrial hyper-acetylation (Lombard et al. 2007). SIRT3 was found to be associated with

18

antioxidant response (Bell and Guarente 2011; Park et al. 2011), regulation of oxidative metabolism, glycolytic pathway (Finley and Haigis 2012), and suppression of mitophagy (Liang et al. 2013; Pi et al. 2015).

In cancer cells energy production relies on glycolysis, instead of mitochondria oxidative phosphorylation. It has been reported that mitochondrial function is essential for the production of key biosynthetic intermediates instead of ATP, directly contributing to cancer cell survival and tumorigenesis (Finley and Haigis 2012). This study investigated the role of SIRT3 in suppressing mitophagy, contributing to cell survival and tumorigenesis of Cr(VI)-transformed cells.

2.3 Material and Methods

2.3.1 Chemicals and reagents

Sodium dichromate dehydrate ($Na_2Cr_2O_7$) and carbonyl cyanide m-chloro phenyl hydrazine (cccp) were obtained from Sigma (St Louis, MO). Dulbecco's modified Eagle's medium (DMEM), fetal bovine serum (FBS), and pen-strep-glutamine solution were obtained from Gibco (Grand Island, NY). shRNAs and overexpressing vectors of SIRT3 and Nrf2 and primers for Real Time PCR were obtained from Origene (Rockville, MD). mKeima-Red-Mito-7 plasmid and PCD FL0X luciferase reporter were from Addgene. RNAeasy mini kit and plasmid prep kit were obtained from Qiagen (Valencia, CA). M-MLV reverse transcriptase and luciferase assay reagents were obtained from Promega (Madison, WI). AccuPrime TaqDNA polymerase high fidelity, antibodies against Alexa Fluor 488 goat anti-mouse IgG1 and Alexa Fluor 649 goat anti-rabbit IgG1, Lipofectamine 2000, and 10-N-Acridine Orange (NAO) were from Invitrogen (Carlsbad, CA). iQ SyBr green supermix was obtained from Bio-Rad (Hercules, CA). Antibodies against SIRT3, p62, p-p62^{Ser349}, Parkin, Pink1, and cytochrome c were obtained from Cell Signaling (Danvers, MA). Antibodies against Nrf2, GAPDH, and Keap-1 were obtained from Santa Cruz Biotechnology (Dallas, TX). Mitochondrial isolation kit and Pierce agarose chip kit were obtained from Thermo Scientific (Waltham, MA). JC-1 mitochondrial membrane potential assay kit was obtained from Cayman Chemical Company (Ann Arbor, MI). Matrigel was obtained from BD Biosciences (San Jose, CA). Chemiluminescence reagent was obtained from Amershan Biosciences (Little Chalfont, United Kingdom).

2.3.2 Cell culture and generation of Cr(VI)-transformed cells

Human bronchial epithelial cells (BEAS-2B) were purchased from the American Type Culture Collection (Rockville, MD). Malignantly transformed cells induced by chronic exposure to Cr(VI) were generated as previously described

(Kim et al. 2015a). Passage-matched BEAS-2B and Cr(VI)-transformed cells were maintained in DMEM supplemented with 10% FBS and 1% pen-strep-glutamine solution at 37 °C and 5% CO_2.

2.3.3 Detection of mitochondria ATP production and proton leak

Cells were seeded in 96-well plates for overnight. Mitochondrial ATP production and proton leak were detected using Seahorse FX mitochondria stress test.

2.3.4 Immunoblotting assay

Cells were harvested, and pellets were lysed in RIPA buffer. Protein concentration was measured using Bradford assay. 30 µg of protein was separated by SDS-PAGE and incubated with primary and secondary antibodies. Chemiluminescence reagent was used to detect protein levels.

2.3.5 Plasmid transfection and establishment of stable knockdown or expressing cells

Transfection was performed using Lipofectamine 2000 as described by the manufacturer's protocol. Briefly, 1.5×10^6 cells were seeded and grown overnight. The cells were transfected with 4 µg of plasmid and selected using DMEM medium containing 2 µg/ml of puromycin for two months. Expression levels of those proteins were detected using immunoblotting analysis.

2.3.6 Real Time PCR

RNeasy mini kit was used to extract and to purify RNA from cultured cells. 0.5 µg of purified RNA was reversed transcribed using qScript cDNA synthesis kit. Following primers were used: SIRT3, 5'-ACCCAGTGGCATTCCAGAC-3' and 5'-GGCTTGGGGTTGTGAAAGAA-3'; NQO1, 5'-TGGAAGTCGTCCCAAGAGA-3' and 5'-TGTCTCCCCAGGACTCTCTCAG-3'; and GAPDH, 5'-

21

GAGTCAACGGATTTGGTCGT-3' and 5'-GACAAGCTTCCCGTTCTCAG-3'. qPCR was performed using Sybr Green mixture in CFX96 Real-time PCR Detection System (Bio-Rad) and data was analyzed using CFX manager software (Bio-Rad).

2.3.7 Mitochondrial isolation

Passage-matched normal BEAS-2B cells and Cr(VI)-transformed cells were grown in cell culture medium. Mitochondrial and cytosolic isolation was performed using the mitochondrial isolation kit following the manufacturers protocol. Mitochondria lysis was performed using 2% CHAPS in tris-buffered saline. 30 µg of protein from cytosolic and mitochondrial fraction were used for immunoblotting analysis.

2.3.8 Detection of mitochondria membrane potential

Mitochondria membrane potential was detected using JC-1 mitochondrial membrane potential assay kit as described by the manufacturer's protocol. Briefly, 10^4 cells were seeded overnight in CO_2 in incubator. The cells were treated with 5 µM of cccp for 4 h. J-aggregates fluorescent intensity was measured using Gemini XPS fluorescence microplate spectrophotometer (Molecular Devices).

2.3.9 Mitochondria mass analysis

Mitochondria mass was measured by staining the cells with 5 µM of 10-N-Acridine Orange (NAO) for 10 min. NAO is a fluorescent probe that stains mitochondria independently of its energetic state (Ferlini and Scambia 2007; Lee et al. 2000; Maftah et al. 1989). Cells were seeded for overnight and treated with 5 µM of cccp for 4 h followed by incubation with 5 µM of NAO for 10 min. NAO fluorescence intensity was measured using Gemini XPS fluorescence microplate spectrophotometer (Molecular Devices).

2.3.10 Mito-keima mitophagy assay

Mito-keima-Red-Mito-7 plasmid was transfected to the cells as described in previous section. Cells were seeded overnight. Lysosomal mKeima fluorescence intensity was measured using dual-excitation radiometric pH measurements at 488 nm (pH 7) and 561 nm (pH 4) lasers with emission filters set for 620 nm and 614 nm, respectively (Lazarou et al. 2015), using Gemini XPS fluorescence microplate spectrophotometer (Molecular Devices).

2.3.11 Immunoprecipitation analysis

Cell lysates were incubated with pre-cleaned beads and centrifuged. Supernatants were collected and incubated with 5 µg of primary antibody for overnight. After incubation with pre-cleaned beads, the samples were washed with PBS and centrifuged followed by adding Laemmli sample buffer. The samples were centrifuged, and supernatant was collected for immunoblotting analysis.

2.3.12 Fluorescence immunocytochemistry analysis

Cells were seeded on the chamber slides for overnight, washed with PBS, and fixed with 4% formaldehyde followed by incubation with 1% Triton-X100. The cells were then incubated with 10% horse serum. Primary antibodies were added and incubated for overnight followed by incubation with secondary antibodies. The slides were mounted with Vectashield mounting medium and visualized using Olympus BX53 fluorescence microscope (Center Valley, PA). Relative colocalization was measured using CellSens Dimension software (Olympus corporation).

2.3.13 Chromatin immunoprecipitation (ChIP) assay

ChIP assay was performed using Pierce^{TM} agarose chip kit. DNA and protein were cross-linked using 1% formaldehyde. The cells were lysed and nuclei was digested with micrococcal nuclease. Chromatin was diluted and immunoprecipitated with 2 µg of Nrf2 antibody or IgG antibody. DNA-protein complexes were eluted from the protein A/G-agarose beads. Binding of Nrf2 to ARE of SIRT3 promoter was analyzed by Real Time PCR. Amplified DNA were separated on 2% agarose gel with Gel Red® followed by band visualization under ultraviolet transillumination.

2.3.14 Luciferase assay

Cells were transfected with 4 µg of SIRT3 luciferase reporter for 48 h. Luciferase activities were measured using Glomax luminometer (Promega). Data were normalized to total cell count.

2.3.15 Tumorigenesis assay

Female athymic nude mice (6-8 weeks old) were purchased from The Jackson Laboratories (Bar Harbor, ME) and housed in sterilized filter-topped cages in a pathogen free animal facility at the Chandler Medical Center, University of Kentucky. Animals were handled according to the Institutional Animal Care and Use Committee (IACUC) guidelines. Cells in 100 µL mixture of DMEM and Matrigel (BD Biosciences) were subcutaneously (*s.c.*) injected on the flank of each mouse. After 3 weeks, mice were euthanized using CO_2 and the tumors were isolated. Tumor weight was measured, and volume was calculated using the formula: (length x width^2)/2.

2.4 Results

2.4.1 SIRT3 positively regulates mitochondrial oxidative phosphorylation pathway in Cr(VI)-transformed cells

In Cr(VI)-transformed cells both protein and mRNA levels of SIRT3 were elevated (Figures 2.1A and 2.1B). Our recent study using RNA sequencing transcriptome analysis demonstrated that all five mitochondrial oxidative phosphorylation complexes were reduced in Cr(VI)-transformed cells compared to passage-matched normal BEAS-2B cells (Clementino et al. 2018). These results are consistent with the results from mitochondrial stress test confirming that mitochondrial ATP production and proton leak were reduced in Cr(VI)-transformed cells (Figures 2.1C and 2.1D). These results suggest that mitochondrial ATP production is inhibited and mitochondrial oxidative phosphorylation pathway is defective in Cr(VI)-transformed cells. To investigate whether SIRT3 is involved in reduced mitochondrial ATP production in Cr(VI)-transformed cells, SIRT3 was inhibited using its shRNA (Figure 2.1E). The results showed that depletion of SIRT3 decreased both mitochondrial ATP production and proton leak in Cr(VI)-transformed cells (Figures 2.1F and 2.1G), indicating that SIRT3 positively regulates mitochondrial oxidative phosphorylation pathway in Cr(VI)-transformed cells.

2.4.2 SIRT3 is a negative regulator of mitophagy in Cr(VI)-transformed cells

Mitochondria mass was reduced in Cr(VI)-transformed cells compared to that in passage-matched normal BEAS-2B cells (Figure 2.2A). There was no observable difference in mitochondria membrane potential (MMP) between passage-matched normal BEAS-2B cells and Cr(VI)-transformed cells (Figure 2.2B), leading to hypothesize that in Cr(VI)-transformed cells mitophagy is suppressed and that upregulation of SIRT3 is responsible for the mitophagy suppression. Our results showed that SIRT3 knockdown decreased

25

mitochondrial membrane potential (MMP) (Figure 2.2E) and further reduced mitochondrial mass (Figure 2.2D). Carbonyl cyanide m-chloro phenyl hydrazine (cccp), a mitochondrial depolarizing agent known to induce mitophagy (Ni et al. 2015; Wei et al. 2015), was used as a positive control. These results suggest that in Cr(VI)-transformed cells, upregulation of SIRT3 prevents mitochondria membrane potential from reduction.

In Cr(VI)-transformed cells, both Pink1 and Parkin were upregulated (Figure 2.2E). SIRT3 was localized in the mitochondria and Parkin was in the cytosol (Figure 2.2G), which ascertains that mitophagy was suppressed in Cr(VI)-transformed cells. Additionally, we observed that SIRT3 knockdown reduced protein levels of Parkin and Pink1 (Figure 2.2G) and translocated Parkin to the mitochondria (Figure 2.2H). The results from Mito-keima analysis showed no difference in mitophagy between Cr(VI)-transformed cells and their passage-matched normal BEAS-2B, whereas knockdown of SIRT3 induced mitophagy in Cr(VI)-transformed cells (Figure 2.2I). Not surprising, treatment with cccp induced mitophagy in both normal BEAS-2B and Cr(VI)-transformed cells. Next, mitophagy was measured under starvation condition. The results showed that under starvation mitophagy was induced in passage-matched normal BEAS-2B cells, but not in Cr(VI)-transformed cells (Figure 2.2J). These results indicate that SIRT3 suppresses mitophagy in Cr(VI)-transformed cells via stabilization of mitochondrial membrane potential.

2.4.3 Upregulation of SIRT3 elevates p62 and Nrf2, leading to increased cell proliferation and tumorigenesis of Cr(VI)-transformed cells

Nrf2, p62 and p-p62^{ser349} levels were all increased in Cr(VI)-transformed cells (Figure 2.3A). SIRT3 knockdown decreased levels of Nrf2, p62, and p-p62^{ser349} (Figure 2.3B) and caused translocation of p62 from cytosol to mitochondria (Figure 2.3C). The results from Figure 2.2I showed that SIRT3 knockdown increased mitophagy in Cr(VI)-transformed cells. These results suggest that upregulation of SIRT3 prevents p62 from mitophagic degradation

through stabilization of mitochondrial membrane potential. Keap1 binds and ubiquitinates Nrf2, targeting to proteasomal degradation of Nrf2 (Suzuki et al. 2016). Keap1 has higher affinity to bind to p-p62^{ser349} than Nrf2 (Ichimura et al. ; Katsuragi et al. 2016a). SIRT3 knockdown or treatment with cccp caused a reduced binding between Keap1 and p-p62^{ser349} and an increased binding between Keap1 and Nrf2, resulting in decreased level of Nrf2 in Cr(VI)-transformed cells (Figure 2.3D), demonstrating that SIRT3 regulates Nrf2 through increased binding of p62 to Keap-1.

We investigated whether upregulation of SIRT3 is essential for increased cell proliferation and tumorigenesis of Cr(VI)-transformed cells. The results showed that inhibition of SIRT3 reduced cell proliferation of Cr(VI)-transformed cells (Figure 2.3E). The results from *in vivo* xenograft tumor growth assay showed that in Cr(VI)-transformed cells 4 out 4 animals (100%) grew tumors and in SIRT3 knockdown cells 1 out of 4 animals (25%) grew tumor (Figure 2.3F). Moreover, tumors isolated from Cr(VI)-transformed cells were heavier (Figure 2.3G) and bigger (Figure 2.3H) than those isolated from SIRT3 knockdown cells. The results from immunoblotting analysis showed the protein levels of Nrf2, p62, and SIRT3 were all markedly reduced in the tumor tissues from SIRT3 knockdown cells compared to those from Cr(VI)-transformed cells (Figure 2.3I). These results demonstrated that SIRT3 plays an important role in the cell proliferation and tumorigenesis of Cr(VI)-transformed cells.

2.4.4 Nrf2 regulates SIRT3 through direct binding to the ARE of SIRT3 gene promoter

Nrf2 knockdown decreased levels of SIRT3, p62 and Parkin in Cr(VI)-transformed cells (Figure 2.4A). SIRT3 overexpression prevented these reductions by Nrf2 knockdown, indicating that Nrf2 is an upstream regulator of SIRT3. Inhibition of Nrf2 also reduced MMP (Figure 2.4B) and mitochondrial mass (Figure 2.4C). SIRT3 overexpression was able to partially restore MMP and mitochondrial mass reduced by Nrf2 inhibition (Figures 2.4B and 2.4C).

Stably expressing Nrf2 in normal BEAS-2B cells was established and the results showed that SIRT3 level was elevated in these Nrf2-expressing BEAS-2B cells (Figure 2.4D), suggesting that regulation of Nrf2 on SIRT3 is not specific for Cr(VI)-transformed cells. Next, we explored the mechanism of regulation of Nrf2 on SIRT3. Both SIRT3 mRNA level and promoter activities were elevated in Nrf2-expressing normal BEAS-2B cells and Cr(VI)-transformed cells compared to those in normal BEAS-2B cells (Figures 2.4E and 2.4F). Nrf2 overexpression in normal BEAS-2B cells increased SIRT3 in both cytosol and nucleus and knockdown of Nrf2 by its shRNA in Cr(VI)-transformed cells reduced SIRT3 in nucleus (Figure 2.4G), suggesting that regulation of Nrf2 on SIRT3 maybe through transcription level. We analyzed human promoter sequence of SIRT3 gene using the transcriptional regulatory element database and identified the antioxidant response element (ARE) of SIRT3 gene promoter (Figure 2.4H). Next, we conducted DNA ChIP assay. The results showed that in normal BEAS-2B cells with Nrf2 overexpression, the binding of Nrf2 to ARE of SIRT3 promoter was markedly increased (Figures 2.4I and 2.4K). In Cr(VI)-transformed cells, knockdown of Nrf2 by its shRNA dramatically reduced the binding of Nrf2 to ARE of SIRT3 gene promoter (Figures 2.4J and 2.4K), demonstrating that Nrf2 regulates SIRT3 through direct binding to the ARE of SIRT3 promoter.

2.4.5   Constitutive activation of SIRT3 is tumorigenic

From the above results we postulated that constitutive activation of SIRT3 is tumorigenic. To begin, we stably expressing SIRT3 in normal BEAS-2B cells. Two clones from these cells were selected and grown. Overexpression of SIRT3 in normal BEAS-2B cells increased protein levels of Nrf2, p62, p-p62^{ser349}, and Parkin (Figure 2.5A). Additionally, SIRT3 was mainly located in mitochondria and Parkin was in the cytosol (Figure 2.5B). As expected, overexpression of SIRT3 suppressed mitophagy (Figure 2.5C). Similar to those in Cr(VI)-transformed cells, forced expression of SIRT3 in normal BEAS-2B cells reduced both mitochondrial ATP production and proton leak (Figures 2.5D and 2.5E). Moreover, overexpression of SIRT3 in normal BEAS-2B cells promoted cell growth, similar

as that in Cr(VI)-transformed cells (Figure 2.5F). The results from *in vivo* tumor growth showed that the animals injected with normal BEAS-2B cells with SIRT3 overexpression grew tumors (3 out of 4 animals in one clone of SIRT3 cells and 4 out 4 animals in another clone of SIRT3 cells) (Figures 2.5G, 2.5H, and 2.5I). The results from immunoblotting analysis showed that these tumor tissues have high levels of Nrf2, p62, p-p62^{ser349}, and Parkin (Figure 2.5J), which are similar as those in Cr(VI)-transformed cells. The above observations demonstrated that constitutive activation of SIRT3 is tumorigenic.

2.5   Discussion

Mitochondrial quality control is required for the maintenance of proper functioning mitochondrial network and cellular metabolism, and for the prevention of accumulation of ROS. Given the pivotal role of mitochondria in cellular homeostasis, defective mitophagy is known to contribute to various diseases. Our previous study has demonstrated that Cr(VI)-transformed cells undergo metabolic reprogramming (Clementino et al. 2018). Cancer cells shift ATP synthesis from oxidative phosphorylation to glycolysis to produce key biosynthetic intermediates in the mitochondria instead of ATP (Finley and Haigis 2012). Therefore, mitochondrial function is essential for cancer cell proliferation and survival. We observed that in Cr(VI)-transformed cells both mitochondrial ATP production and proton leak were markedly reduced. The extent of these reductions may depend on the malignancy or aggressiveness of these transformed cells. We noted that mitochondrial function may be moderately or not affected in Cr(VI)-transformed cells with less malignancy or aggressiveness. The Cr(VI)-transformed cells used in the present study are considered as aggressive ones as evidenced by (1) high resistance to apoptosis; (2) rapid cell proliferation; (3) rapid tumor growth (reaching maximum tumor volume within 3 weeks post injection of 10^6 cells in the nude mice). In addition, we used adenocarcinomic human alveolar basal epithelial A549 cells to detect the mitochondrial function. Similar results were obtained as those in Cr(VI)-transformed cells. SIRT3 regulates metabolic homeostasis via deacetylation of mitochondrial proteins (Finley and Haigis 2012; Giralt and Villarroya 2012). In human cancer cells, mutant SIRT3 reduces mitochondrial membrane potential and mitochondrial ATP generation (Liu et al. 2015). SIRT3 regulates oxidative phosphorylation (OXPHOS) at different levels. SIRT3 regulates activities of complexes I and III via deacetylation of these complexes' subunits (Ahn et al. 2008; Cimen et al. 2010). Once complexes I and III are deacetylated by SIRT3 they produce less ROS, therefore working more efficiently (Ahn et al. 2008; Cimen et al. 2010; Finley and Haigis 2012). Additionally, SIRT3 regulates

enzymes involved in The Citric Acid (TCA) cycle. It has been reported that SIRT3 deacetylates succinate dehydrogenase (SDH) (Finley et al. 2011) and isocytrate dehydrogenase 2 (IDH2) (Someya et al. 2010). SDH participates in both the TCA cycle and electron transport chain, therefore it is well situated to coordinate flux through both pathways (Finley et al. 2011). IDH2 provides reducing equivalents to combat oxidative stress or to promote anabolic reactions by reducing NADP to NADPH (Someya et al. 2010). Deacetylation of SDH and IDH2 by SIRT3 could potentially stimulate mitochondria oxidative capacity and protect cells against oxidative stress. Thus, SIRT3 is expected to play decisive role in cell survival and cell response to stress. Tumors harboring mutant SIRT3 exhibit inhibited tumor growth and increased sensitivity to local radiation in vivo (Liu et al. 2015). The present study we observed that SIRT3 is constitutively activated in Cr(VI)-transformed cells; that this constitutively activated SIRT3 is essential in the maintenance of mitochondrial function; contributes to cell survival and tumorigenesis of Cr(VI)-transformed cells. In summary these results show that constitutive activation of SIRT3 is tumorigenic.

Mitochondrial membrane potential and mitochondria mass are two indicators of mitochondrial integrity. PINK1 accumulates in damaged mitochondria, which in turn recruits Parkin, resulting in ubiquitination of mitochondrial proteins (Ivankovic et al. 2016). Previous studies have shown that upregulation of SIRT3 stabilizes MMP and maintains mitochondrial mass (Pellegrini et al. 2012; Yang et al. 2016; Zhang et al. 2016b). Our results showed that in Cr(VI)-transformed cells SIRT3 was constitutively activated, MMP remained unchanged, and mitochondrial mass was reduced compared to those in passage-matched normal BEAS-2B cells. Knockdown of SIRT3 by its shRNA decreased MMP and further reduced mitochondria mass. Thus we speculated that constitutive activation of SIRT3 is essential to maintain MMP and mitochondrial function in Cr(VI)-transformed cells. Under normal condition, mitophagy remained similar between normal BEAS-2B cells and Cr(VI)-transformed cells. However, starvation was able to induce mitophagy in normal BEAS-2B cells, but not in Cr(VI)-transformed cells, indicating that mitophagy is

defective in Cr(VI)-transformed cells. Mitochondria membrane depolarization is the first step to induce mitophagy. Once MMP is reduced, Pink1 recruits Parkin to the mitochondria. Under the conditions which mitochondria are undamaged, Pink1 is imported into the mitochondrial inner membrane, where Pink1 is cleaved. Aberration in mitochondrial membrane potential impairs import of Pink1 to the mitochondrial inner membrane, leading to the stabilization of Pink1 on the mitochondrial outer membrane (Bernardini et al. 2017). Parkin is responsible to target this organelle to autophagosomal destruction (Durcan and Fon 2015; Eiyama and Okamoto 2015; Lazarou et al. 2015; Ni et al. 2015). We have observed that both Pink1 and Parkin levels were elevated in Cr(I)-transformed cells and Parkin was mainly located in the cytoplasm, providing the explanation of defective mitophagy in Cr(VI)-transformed cells.

It has been reported that SIRT3 regulates mitophagy machinery proteins Parkin and Pink1 (Das et al. 2014; Liang et al. 2013; Pi et al. 2015; Qiao et al. 2016; Yu et al. 2016). We speculated that constitutively activated SIRT3 contributes to the defective mitophagy in Cr(VI)-transformed cells. The results showed that in Cr(VI)-transformed cells inhibition of SIRT3 induced mitochondria membrane depolarization, translocated Parkin from cytosol to the mitochondria, and restored mitophagy. Thus we conclude that constitutively activated SIRT3 may contribute to mitophagy deficiency of Cr(VI)-transformed cells.

It has been reported that recruitment of autophagic adaptor p62/SQSTM1 to the mitochondrial clusters is essential for the clearance of mitochondria (Geisler et al. 2010). p62 interacts with the autophagosome membrane to target the mitochondria to undergo autophagosomal destruction (Chourasia et al. 2015; Ding and Yin 2012; Kulikov et al. 2017; Ni et al. 2015; Wei et al. 2015). We observed that p62 was upregulated in Cr(VI)-transformed cells. p62 was mainly located in the surrounding area of mitochondria, thus blocking the degradation of damaged mitochondria in Cr(VI)-transformed cells. Inhibition of SIRT3 caused translocation of p62 to the mitochondria, promoting mitochondrial degradation through autophagosome and mitophagy induction.

Nrf2 is a key transcription factor that regulates antioxidant proteins to neutralize ROS and to restore cellular redox balance (Lee et al. 2012; Niture et al. 2010; Zhang et al. 2015a). ROS play a major role in metal-induced carcinogenesis (Kim et al. 2015a; Kim et al. 2016; Lee and Yu 2016; Lee et al. 2012; Pratheeshkumar et al. 2016; Son et al. 2014; Zhang et al. 2015b). Inducible Nrf2 decreases carcinogenesis in the early stage via decrease of oxidative stress (Sporn and Liby 2012), constitutively activated Nrf2 exerts oncogenic effects by protecting cancer cells from oxidative stress and chemotherapeutics (Kansanen et al. 2013a; Wang et al. 2008). Recent studies have highlighted its role in mitochondrial function, including regulation of mitophagy via interaction with p62 and Keap1 (Dinkova-Kostova and Abramov 2015; Holmström et al. 2017). Our results showed that Nrf2 is constitutive activated in Cr(VI)-transformed cells. Knockdown of Nrf2 reduced SIRT3 protein level, mitochondria mass, and MMP. However, overexpression of SIRT3 partially prevents reduction of both mitochondria mass and MMP by Nrf2 knockdown. These results demonstrate that SIRT3 is downstream target of Nrf2 signaling in regulation of mitophagy in Cr(VI)-transformed cells. Previous study showed that Nrf2 induced SIRT3 expression in 293T cells (Satterstrom et al. 2015). The present study has demonstrated that Nrf2 positively regulates SIRT3 in Cr(VI)-transformed cells via directly binding to the ARE of SIRT3 gene promoter. Cr(VI) induces ROS generation, activating a cellular response to prevent the generation of ROS or detoxify ROS. The activation of Nrf2 pathway is considered to be the most important for cell survival during oxidative stress (Niture et al. 2010). Nrf2 activates the expression of several antioxidant enzymes by directly biding to the ARE of their gene promoters (Niture et al. 2010). Our results showed that in Cr(VI)-transformed cells activation of Nrf2 causes upregulation of SIRT3, SIRT3 upregulation acts to promote cancer cell survival and tumorigenesis. It has been reported that Nrf2 regulates p62 via direct its binding to the ARE of p62 gene promoter (Katsuragi et al. 2016b). p62 feedbacks to Nrf2 via competitive binding to the Keap1 (Jain et al. 2010). In the agreement of these findings, the present study has demonstrated that upregulation of p-p62[Ser349] in Cr(VI)-transformed

cells competitively binds to Keap1 with Nrf2, resulting in reduced binding of Keap1 to Nrf2 and subsequently elevated Nrf2. Inhibition of SIRT3 decreased p-p62^{Ser349}, leading to increased binding of Keap1 to Nrf2, subsequently decreased Nrf2. Human adenocarcinomic epithelial A549 cells were also used to examine the effects of SIRT3 on Nrf2/p62, Pink1/Parkin, and mitochondrial functions. The similar results as those in Cr(VI)-transformed cells were obtained (Suppl figure 1). In summary, these results suggest that in Cr(VI)-transformed cells (1) Nrf2 positively regulates SIRT3 via its direct binding to ARE of SIRT3 promoter; (2) p62^{Ser349} binds to Keap1, resulting in upregulation of Nrf2; and (3) SIRT3 feedbacks to Nrf2 via interacting with Keap1-Nrf2/p62 pathway.

In Cr(VI)-transformed cells SIRT3 is upregulated. Inhibition of SIRT3 reduced cell proliferation and tumorigenesis of Cr(VI)-transformed cells, suggesting that SIRT3 maybe tumorigenic. Previous studies reported that SIRT3 had oncogenic properties (Chen et al. 2014; Giralt and Villarroya 2012; Morris et al. 2011; Pillai et al. 2010). Our results showed that forced SIRT3 expression in passage-matched normal BEAS-2B cells increased levels of Nrf2, p62, p-p62^{Ser349}, and Parkin. Our result also showed that forced expression of SIRT3 expression reduced mitochondrial ATP production and proton leak and suppressed mitophagy, which are similar as those in Cr(VI)-transformed cells. Importantly, forced SIRT3 expression in passage-matched normal BEAS-2B cells increased cell proliferation in vitro and caused tumor growth in vivo.

In summary, the present study demonstrated that SIRT3 is essential to maintain mitochondrial basal oxidative phosphorylation of Cr(VI)-transformed cells. Cr(VI)-transformed cells are mitophagy defective. Inhibition of SIRT3 induces mitophagy and decreases proliferation and tumorigenesis of Cr(VI)-transformed cells. Constitutively activated Nrf2 upregulates SIRT3 via its direct binding to ARE of SIRT3 promoter. SIRT3 feedbacks to Nrf2 via interacting Keap1/Nrf2 axis. High level of SIRT3 in normal cells is sufficient to induce tumor growth in xenograft animal model, indicating that SIRT3 is tumorigenic. The

mechanism of SIRT3 in mitophagy and tumorigenesis of Cr(VI)-transformed cells is summarized in Figure 6.
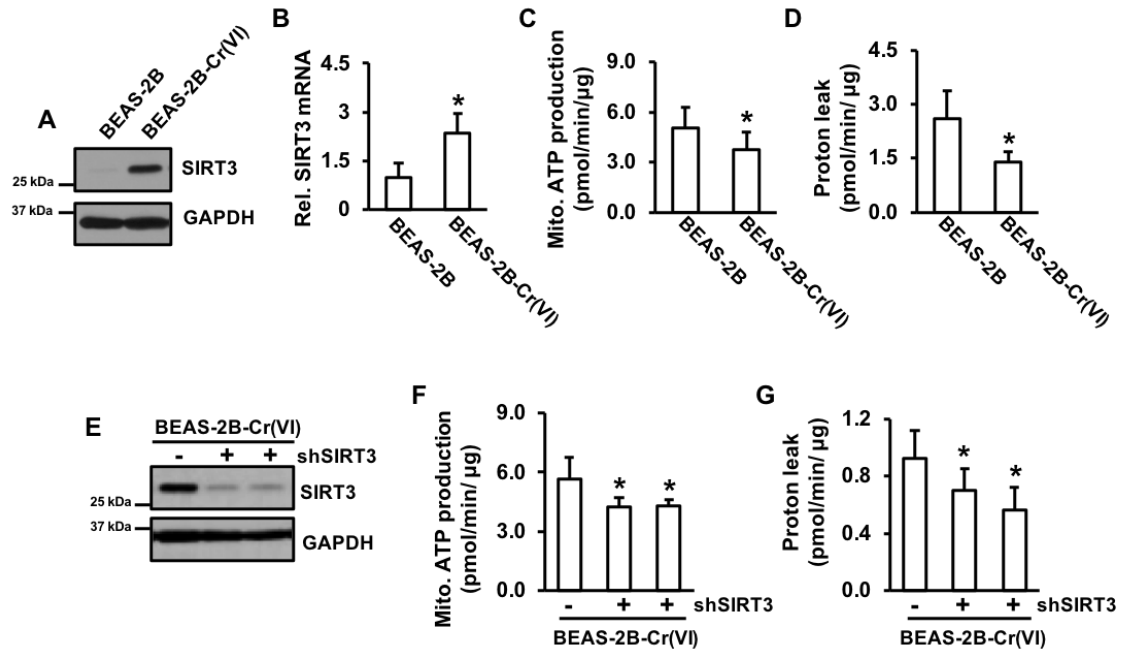
Figure 2.1 **SIRT3 is a positive regulator of mitochondrial oxidative phosphorylation pathway in Cr(VI)-transformed cells.** (A) Whole protein lysates from Cr(VI)-transformed cells and passage-matched normal BEAS-2B were used for immunoblotting analysis. (B) RNA was isolated from BEAS-2B and Cr(VI)-transformed cells and subjected to RT-PCR analysis. (C) and (D) BEAS-2B and Cr(VI)-transformed cells were seeded in 96-well plates for overnight. Mitochondrial stress test was conducted using Seahorse analysis. Data are expressed as mean ± SD (n=8). *, p < 0.05 compared to those in passage-matched BEAS-2B cells. (E) Cr(VI)-transformed cells were transfected with or without shSIRT3. Whole protein lysate were subjected to immunoblotting analysis. (F) and (G) Cr(VI)-transformed cells transfected with or without shSIRT3 were seeded in 96-well plates for overnight followed by mitochondria stress test using Seahorse analysis. Data are expressed as mean ± SD (n=8). *, p < 0.05 compared to Cr(VI)-transformed cells without SIRT3 knockdown.
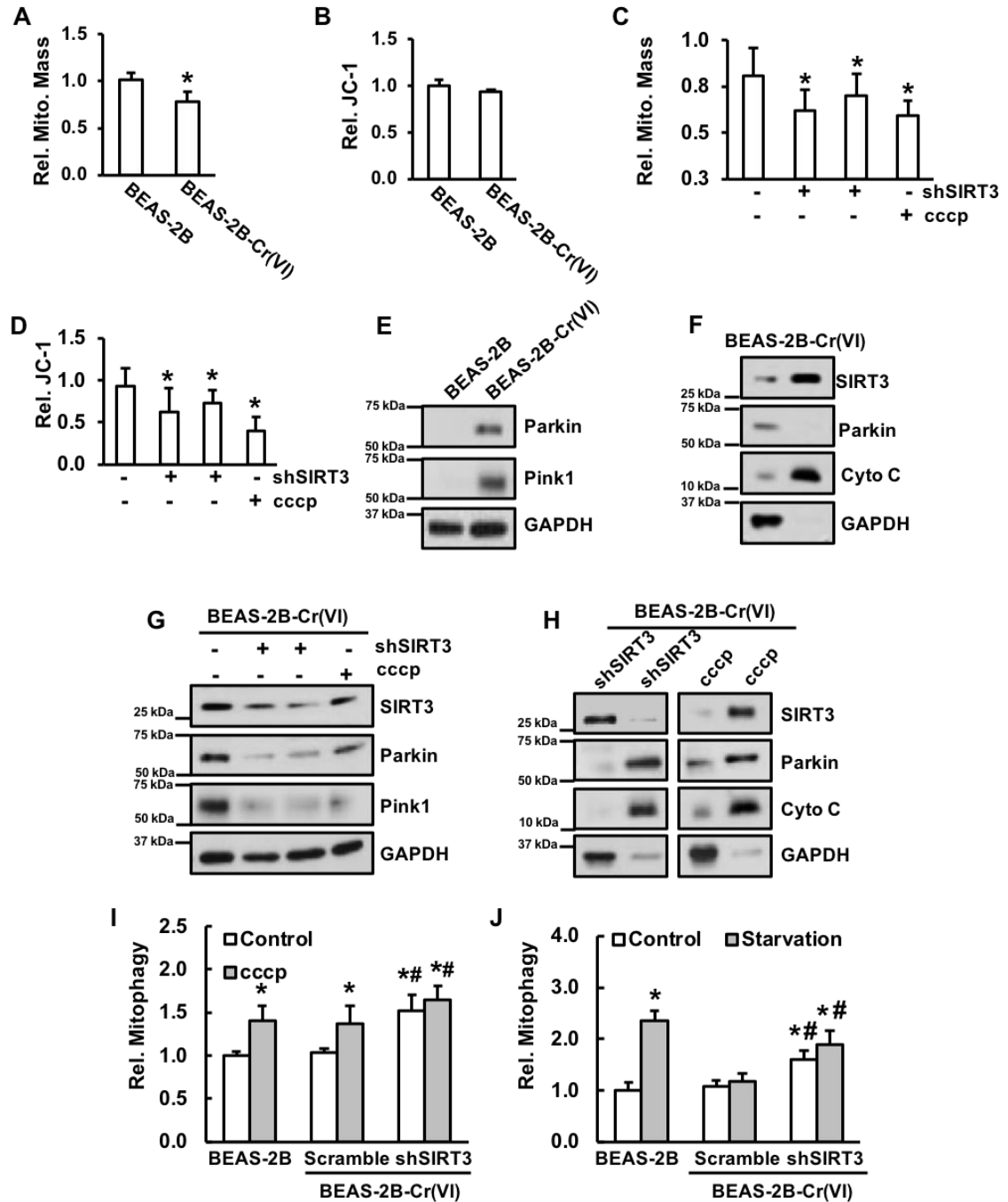
Figure 2.2 **SIRT3 is a negative regulator of mitophagy in Cr(VI)-transformed cells.**
(A) and (B) BEAS-2B and Cr(VI)-transformed cells were seeded in 96-well plate for
overnight. (A) Mitochondrial mass was measured via NAO fluorescence intensity and (B)
JC-1 fluorescence intensity was measured. Data are expressed as mean ± SD (n=8). *,
p < 0.05 compared to that in BEAS-2B cells. (C) and (D) Cr(VI)-transformed cells
transfected with or without shSIRT3, or treated with 5μM of cccp for 4h were seeded in

96-well plate for overnight. (C) Mitochondrial mass was measured via NAO fluorescence intensity and (D) JC-1 fluorescence intensity was measured. Data are expressed as mean ± SD (n=8). *, $p < 0.05$ compared to that in Cr(VI)-transformed cells. (E) Whole protein lysates from Cr(VI)-transformed cells and BEAS-2B were subjected to immunoblotting analysis. (F) Mitochondrial and cytosolic fraction from Cr(VI)-transformed cells were isolated and subjected to immunoblotting analysis. (G) Whole protein lysates from Cr(VI)-transformed cells transfected with or without shSIRT3, or treated with 5μM of cccp for 4h were subjected to immunoblotting analysis. (H) Mitochondrial and cytosolic fraction from Cr(VI)-transformed cells transfected with or without shSIRT3, or treated with 5 μM of cccp for 4h were subjected to immunoblotting analysis. (I) Cr(VI)-transformed cells transfected with or without shSIRT3, or treated with 5 μM of cccp for 4h were seeded in 96-well plate for overnight. mKeima fluorescence intensity in dual-excitation was measured. Data are expressed as mean ± SD (n=8). * and #, $p < 0.05$ compared to that in BEAS-2B cells without cccp treatment or Cr(VI)-transformed cells, respectively. (J) Cr(VI)-transformed cells transfected with or without shSIRT3 were seeded in 96-well plate for overnight. Cells were exposed to starvation condition for 24h. mKeima fluorescence intensity in dual-excitation was measured. Data are expressed as mean ± SD (n=8). *$p < 0.05$ compared to control.
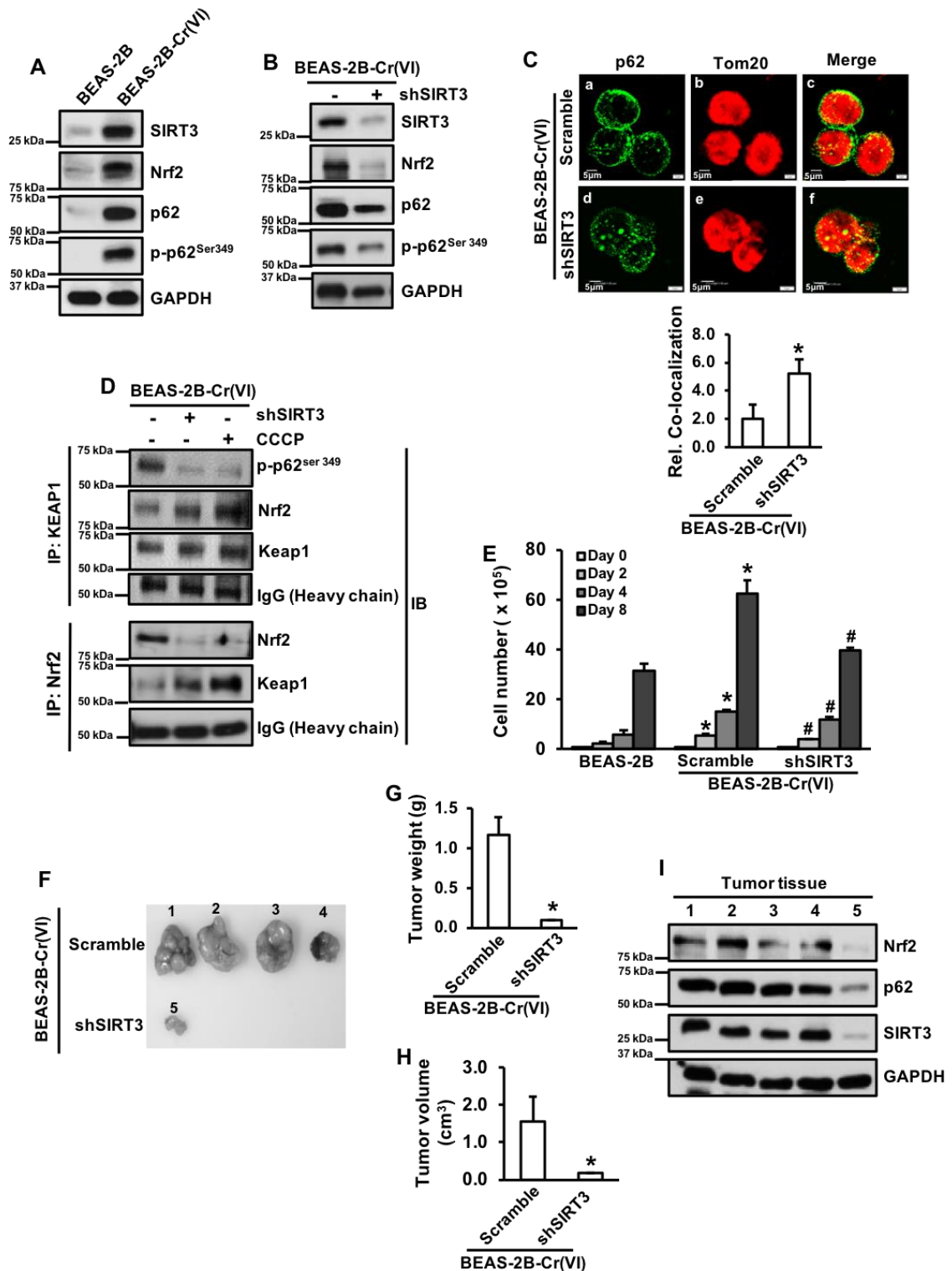
Figure 2.3 **Upregulation of SIRT3 elevates p62 and Nrf2, leading to increased cell proliferation and tumorigenesis of Cr(VI)-transformed cells.** (A) and (B) Whole protein lysates from BEAS-2B and Cr(VI)-transformed cells transfected with or without

shSIRT3 were subjected to immunoblotting analysis. (C) Cr(VI)-transformed cells transfected with or without shSIRT3 were subjected to fluorescence immunohistochemistry analysis. Relative Co-localization was measured using CellSens Dimension software. Images were represented one sample in each treatment group (Left). Fluorescence intensities were quantitated (Right). Data are expressed as mean ± SD (n=3). *, $p < 0.05$, compared to that in Cr(VI)-transformed cells-scramble. (D) Whole protein lysates from Cr(VI)-transformed cells transfected with or without shSIRT3, or treated with 5 μM of cccp for 4h were subjected to co-immunoprecipitation analysis. (E) BEAS-2B and Cr(VI)-transformed cells were seeded in 6-well plates for 2, 4 and 8 days and total cell number was counted. Data are expressed as mean ± SD (n=3). * and #, $p < 0.05$, compared to that in BEAS-2B cells or Cr(VI)-transformed cells, respectively. (F), (G), and (H) 6-8 week old, female immune-deficient mice were subcutaneously injected with Cr(VI)-transformed cells transfected with or without shSIRT3. After 8 weeks, tumor volumes (Length x Width^2/2) were measured (H). Tumor tissues were isolated. Tumors were pictured (F) and weighted (G). Protein lysates were extracted from tumor tissues for immunoblotting analysis (I). (G) and (H), data are expressed as mean ± SD (n=4). *, $p < 0.05$ compared to that in Cr(VI)-transformed cells.
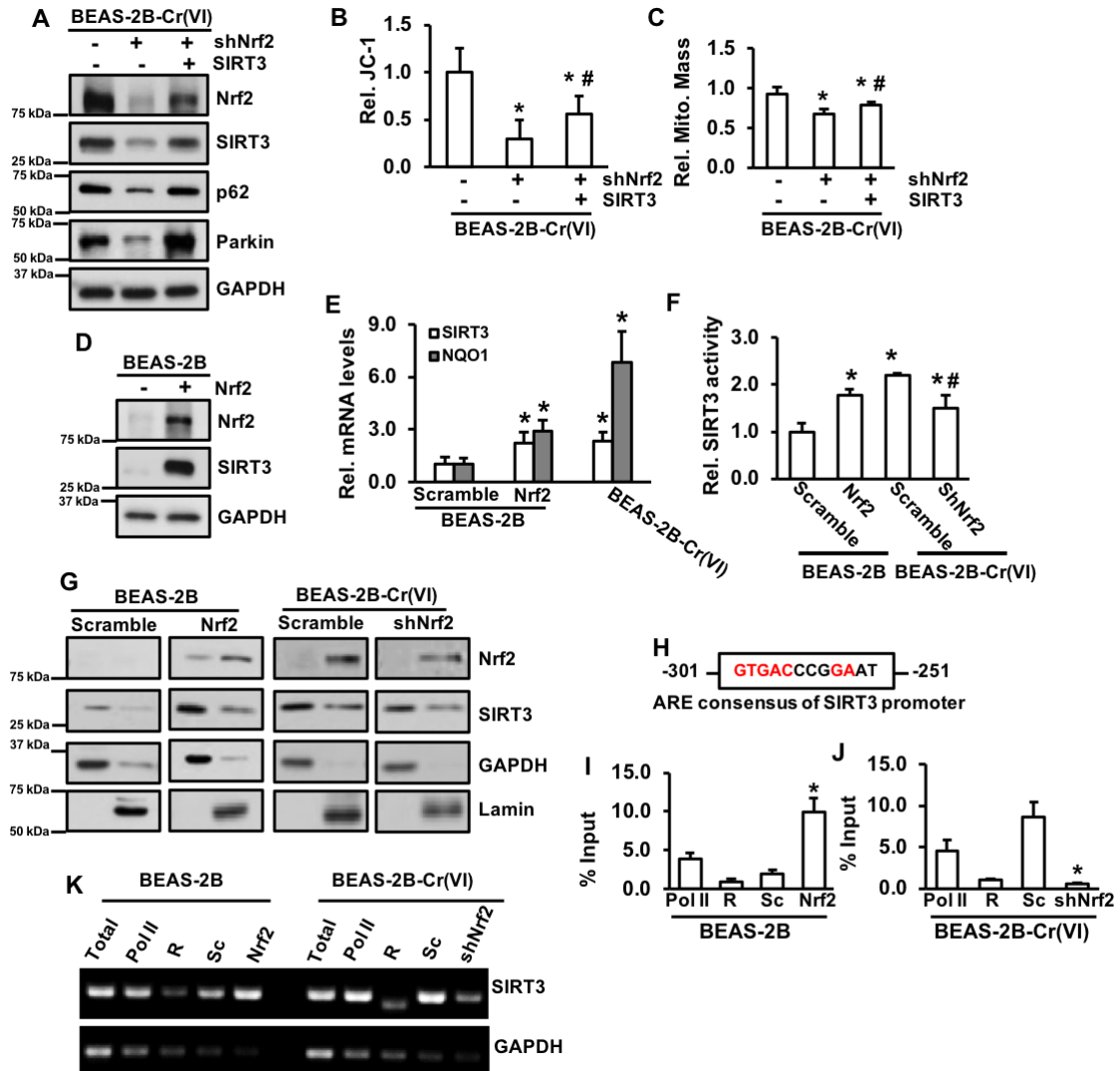
Figure 2.4 **Nrf2 regulates SIRT3 through direct binding to the ARE of SIRT3 gene promoter**. (A), (B), and (C) Cr(VI)-transformed cells transfected with or without shNrf2, or in combination with SIRT3 expression were submitted for immunoblotting analysis (A). (B) JC-1 analysis was performed; (C) Mitochondria mass was measured. (B) and (C) Data are expressed as mean ± SD (n=8). * and #, p < 0.05, compared to those in Cr(VI)-transformed cells and Cr(VI)-transformed cells Nrf2 knockdown, respectively. (D) Whole lysates from BEAS-2B with or without stable Nrf2 expression were subjected to immunoblotting analysis. (E) RNA was isolated from BEAS-2B with or without stable Nrf2 expression. mRNA level was measured using RT-PCR analysis. Data are expressed as mean ± SD (n=8). *, p < 0.05, compared to that in BEAS-2B Scramble cells. (F) BEAS-2B with or without stable Nrf2 expression and Cr(VI)-transformed cells with or without Nrf2 knockdown were transfected with SIRT3 luciferase reporter. After

48h of transfection, the cells were seeded in 96-well plates for overnight, followed by luciferase measurement. Data are expressed as mean ± SD (n=8). * and #, p < 0.05, compared to that in BEAS-2B Scramble cells and Cr(VI)-transformed cells scramble cells, respectively. (G) Nuclear and cytosolic fractions from BEAS-2B with or without stable Nrf2 expression and Cr(VI)-transformed cells with or without Nrf2 knockdown were isolated and subjected to immunoblotting analysis. (H) Consensus of ARE of human SIRT3 gene promoter. (I)-(K) BEAS-2B with or without stable Nrf2 expression and Cr(VI)-transformed cells with or without Nrf2 knockdown were submitted to chromatin immunoprecipitation with anti-Nrf2 antibody or control rabbit IgG. Binding of Nrf2 to SIRT3 promoters was analyzed by PCR using specific primers. GAPDH was used as a control. (I) and (J) ChIP and quantitative (*q*) RT-PCR. The amounts of immunoprecipitated DNA were normalized to the inputs and plotted. Data are mean ± SD (n=3). *, p < 0.05, compared to Scramble cells. (K) Amplified DNA were separated on agarose gel followed by band visualization under ultraviolet transillumination.
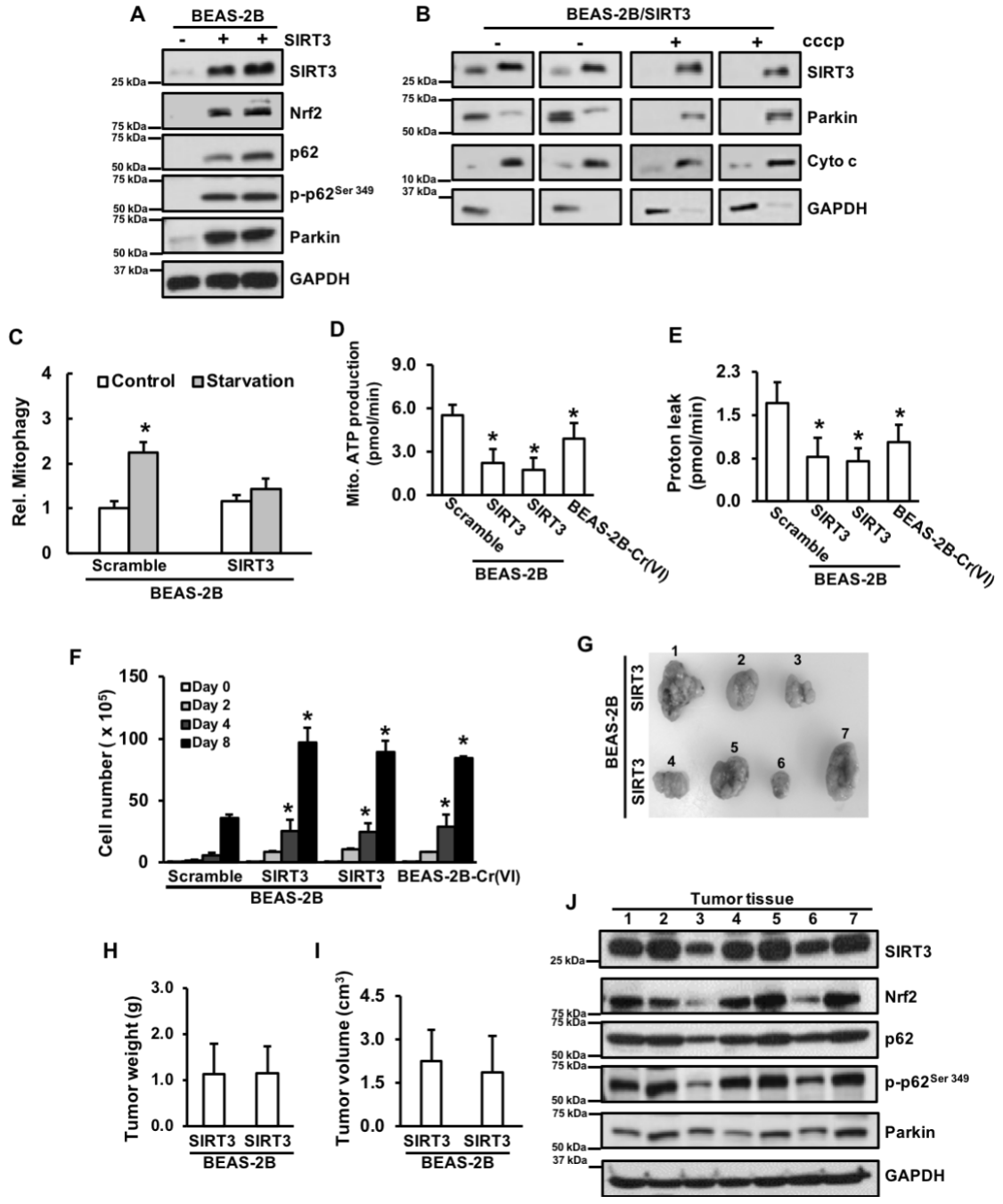
Figure 2.5 **Constitutive activation of SIRT3 is tumorigenic.** (A) BEAS-2B cells were transfected with SIRT3 expression vector. Whole lysates were harvested for immunoblotting analysis. (B) BEAS-2B cells with or without stable expression of SIRT3 were treated with 5 µM of cccp for 4h. Mitochondrial and cytosolic fractions were isolated for immunoblotting analysis. (C) BEAS-2B cells with or without stable expression of

SIRT3 were seeded in 96-well plate for overnight. Cells were exposed to starvation condition for 24h. mKeima fluorescence intensity in dual-excitation was measured. Data are expressed as mean $\pm$ SD (n=8). *, $p < 0.05$, compared to control. (D) and (E) BEAS-2B cells with or without stable expression of SIRT3 were seeded in 96-well plates for overnight. Mitochondrial stress test was conducted using Seahorse analysis. Data are expressed as mean $\pm$ SD (n=8). *, $p < 0.05$, compared to those in BEAS-2B cells. (F) BEAS-2B cells with or without stable expression of SIRT3 were seeded in 6-well plates for 2, 4 and 8 days and total cell number was counted. Data are expressed as mean $\pm$ SD (n=3). *, $p < 0.05$, compared to that in BEAS-2B cells. (G), (H), and (I) 6-8 week old, female immune-deficient mice were subcutaneously injected with BEAS-2B cells with or without SIRT3 stable expression. After 8 weeks, tumor volumes were measured (I). Tumor tissues were isolated. Tumors were pictured (G) and weighted (H). Protein lysates were extracted from tumor tissues for immunoblotting analysis (J).
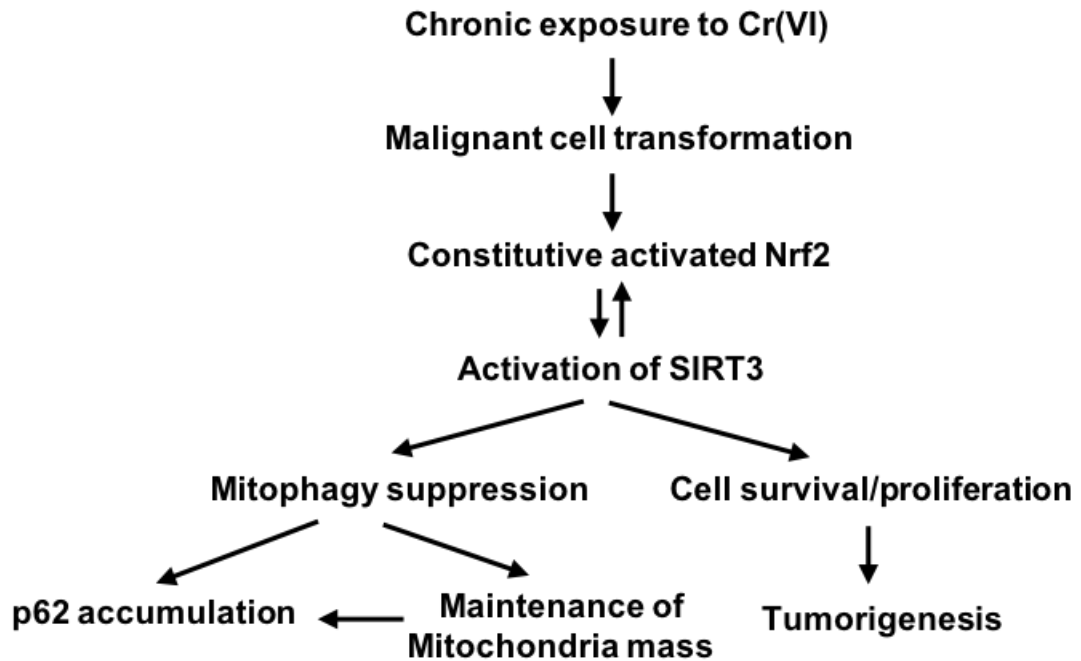
Figure 2.6 **The scheme of mechanism of SIRT3 in mitophagy and tumorigenesis of Cr(VI)-transformed cells.** Chronic exposure of the cells to Cr(VI) at low dose causes malignant cell transformation. The malignantly transformed cells exhibit constitutive activated Nrf2 and SIRT3, leading to mitophagy deficiency, contributing to cell survival and tumorigenesis of Cr(VI)-transformed cells.

CHAPTER 3. Constitutive activation of Nrf2 Induces glycolytic shift in Cr(VI)-transformed Cells

3.1 Abstract

Hexavalent chromium (Cr(VI)) chronic exposure to normal BEAS-2B cells induces cell transformation. Cr(VI)-transformed cells are tumorigenic. Nuclear factor erythroid-(derived 2)-like 2 (Nrf2) is a transcription factor that regulates oxidative stress response. The present study investigated how Nrf2 regulates metabolic reprogramming in Cr(VI)-transformed cells. The results from glycolytic stress test showed that glycolytic ATP production was increased in Cr(VI)-transformed cells compared to that in passage-matched normal BEAS-2B cells. Nrf2 overexpression in normal BEAS-2B cells increased glycolytic ATP production. The results from RNAseq analysis showed that Nrf2 overexpression in normal BEAS-2B cells activated AMPK signaling pathway. The results from immunoblotting analysis confirmed that in Cr(VI)-transformed cells p-AMPK^{Thr172} was elevated. Nrf2 knockdown in Cr(VI)-transformed cells reduced the phosphorylation of AMPK. Nrf2 overexpression in normal BEAS-2B cells increased p-AMPK^{Thr172}. In Cr(VI)-transformed cells AMPK inhibition by its shRNA or treatment with dorsomorphin (5 µM) reduced PFK1 and PFKFB3 protein levels and glycolytic ATP generation. Overall, our results suggested that Nrf2 regulated glycolysis via activation of AMPK pathway. Furthermore, our results showed that forced expression of Nrf2 in BEAS-2B cells increased cell proliferation and tumorigenesis. Knockdown of Nrf2 reduced cell proliferation and tumorigenesis of Cr(VI)-transformed cells. In conclusion, the present study demonstrated that constitutive activation of Nrf2 in Cr(VI)-transformed cells: (1) increased glycolytic ATP generation; (2) activated AMPK signaling pathway; and (3) increased cell proliferation and tumorigenesis.

3.2 Introduction

Hexavalent chromium (Cr(VI)) is classified as a Group 1 human carcinogen by the International Agency for Research in Cancer (IARC). It has been reported that chronic exposure of Cr(VI) at low dosage induced malignant cell transformation of human bronchial epithelial (BEAS-2B) cells and those Cr(VI)-transformed cells are tumorigenic (Kim et al. 2015b).

Cancer cells accumulate distinctive capabilities in order to enable increased cell proliferation, tumor growth and metastatic distribution. To better understand the biology of cancer, ten hallmarks of cancer have been stablished (Hanahan and Weinberg). Previous studies demonstrated the several properties of Cr(VI)-transformed cells, including reduced capacity of generating ROS, increased cell proliferation, increased angiogenesis, and resistance to cell death (Kim et al. 2016; Kim et al. 2015b; Lee et al. 2012; Pratheeshkumar et al. 2016; Wang et al. 2011). A recent review has highlighted the importance of metabolic reprogramming in Cr(VI)-transformed cells (Zhang et al. 2016a).

Our previous study has demonstrated that expressions of genes associated with glycolysis, pentose-phosphate pathway (PPP), and glutaminolysis were elevated in Cr(VI)-transformed cells compared to these in passage-matched normal BEAS-2B cells. In contrast, expressions of genes associated with oxidative phosphorylation (OXPHOS) were downregulated in Cr(VI)-transformed cells (Clementino et al. 2018), suggesting that Cr(VI)-transformed cells undergo deregulation of their cellular energetics, in accordance with the proposed hallmark of cancer (Hanahan and Weinberg) and the Warburg effect (Lu et al. 2015).

Nuclear factor erythroid-(derived 2)-like 2 (Nrf2) is a transcription factor that regulates antioxidants in response to oxidative stress (Kobayashi and Yamamoto 2006). Nrf2 plays dual roles in carcinogenesis. In normal cells inducible Nrf2 decreases oxidative stress and malignant cell transformation (Sporn and Liby 2012). In cancer cells constitutively activated Nrf2 protects the cells from

47

oxidative stress and chemotherapeutics, promoting cell survival (Wang et al. 2008). Nrf2 is constitutively activated in several tumors and cancer cell lines (Lau et al. 2013; Ohta et al. 2008; Sporn and Liby 2012; Tong et al. 2006). High level of Nrf2 is associated with poor prognosis (Shibata et al. 2008; Solis et al. 2010). Nrf2 plays an important role in regulating anabolic metabolism and glucose uptake (Hawkins et al. 2016; Heiss et al. 2013; Mitsuishi et al. 2012; Singh et al. 2008). The present study investigated the role of Nrf2 in the regulation of metabolic reprogramming contributing to tumorigenesis of Cr(VI)-transformed cells.

3.3 Materials and Methods

3.3.1 Chemicals and reagents

Sodium dichromate dehydrate ($Na_2Cr_2O_7$) was obtained from Sigma (St Louis, MO). Dulbecco's modified Eagle's medium (DMEM), fetal bovine serum (FBS), and pen-strep-glutamine solution were obtained from Gibco (Grand Island, NY). shRNAs and overexpressing vectors Nrf2 and AMPKα, and primers for Real Time PCR were obtained from Origene (Rockville, MD). RNAeasy mini kit and plasmid prep kit were obtained from Qiagen (Valencia, CA). Lipofectamine 2000 was from Invitrogen (Carlsbad, CA) Antibodies against Nrf2, hexokinase 2 (HK2), 6-phosphofructo-2-kinase/fructose-2,6-biphosphatase 3 (PFKFB3), AMP-activated protein kinase (AMPK), p-AMPK^{thr172}, glyceraldehyde-3-phosphate dehydrogenase (GAPDH) and superoxide dismutase 2 (SOD2) were obtained from Cell Signaling (Danvers, MA). Antibodies against phosphofructokinase-1 (PFK1) was obtained from Santa Cruz Biotechnology (Dallas, TX). Matrigel was obtained from BD Biosciences (San Jose, CA). Chemiluminescence reagent was obtained from Amershan Biosciences (Little Chalfont, United Kingdom).

3.3.2 Cell culture

Human bronchial epithelial cells (BEAS-2B) purchased from the American Type Culture Collection (ATCC) were maintained as described previously (Kim et al. 2015b). Briefly, passage-match BEAS-2B and Cr(VI)-transformed cells were maintained in DMEM supplemented with 10% FBS and 1% pen-strep-glutamine solution at 37 °C and 5% CO_2. Cr(VI)-transformed cells were generated as described previously (Kim et al. 2015b).

3.3.3 Plasmid transfection and stable cell lines

Transfection was performed using Lipofectamine 2000 as described by the manufacturer's protocol. Briefly, 1.5 million cells were seeded in 6 cm dishes and allowed to grow for overnight. Cells were transfected with 2-4 µg of plasmid. To establish stable cells, after transfection cells were cultured in DMEM media containing 0.02 µg/ml of puromycin for the first week. Puromycin concentration was increased gradually up to 2 µg/ml with 50% concentration increment every week. After two months, single clones were picked up and expression of target proteins was examined using immunoblotting analysis

3.3.4 RNA sequence analysis

RNAeasy mini kit was used to extract and purify RNA. Total RNA of normal BEAS-2B and Cr(VI)-transformed BEAS-2B cells were collected in triplicates. RNA quality was accessed using RNA Nano Chip Kit. Samples with higher than 8 in RNA integrity umber (RIN) were selected. Libraries were prepared following TruSeq® Standart total RNA protocol, followed by whole transcriptome sequencing of 100 bp paired-end reads using HiSeq 2500 Rapid Run at University of Kentucky Genomics Core Laboratory.

3.3.5 RNA sequencing data analysis

Transcriptome of each sample was analyzed using esembl GRCh38 Human Transcriptome as reference. Gene expression was calculated using RSEM (Li and Dewey 2011) and differentially expressed (DE) genes were detected using EBseq (Leng et al. 2015). A false detection rate (FDR) analysis with 0.05 threshold was performed. The lists of DE genes were submitted to ENRICHr for gene ontology enrichment analysis (Kuleshov et al. 2016).

3.3.6 Immunoblotting analysis

Cell pellets were lysed in RIPA buffer. Bradford Assay was used to measure protein concentration. 30 µg of protein was separated by SDS-PAGE followed by incubation with primary and secondary antibodies. Chemiluminescence reagent was used to detect protein bands.

3.3.7 Glycolytic stress tests

Glycolytic stress test was performed in a Seahorse 96-well XF cell culture microplate in conjunction with an XF96 sensor cartridge. 80 µL of growth medium containing 40,000 cells were seeded for overnight. The plate was submitted for glycolysis analysis.

3.3.8 In vivo Tumorigenesis assay

Female athymic nude mice (6-8 weeks old) were purchased from Jackson Laboratories (Bar Harbor, ME). Animals were handled according to guidelines provided by the Institutional Animal Care and Use Committee (IACUC). Animals were housed in sterilized filter-topped cages in a pathogen free animal facility and the Chandler Medical Center, University of Kentucky. 100 µL mixture of DMEM, Matrigel (BD Biosciences) and cells were subcutaneously (*s.c*) injected on the flank of each mouse. 3 weeks after injection, mice were euthanized using CO_2. The tumors were isolated, and pictures were captured. Both tumor volume and weight were measured. Tumor volume was calculated using the following formula: (length x width^2)/2.

3.4   Results

3.4.1   Increased glycolysis in Cr(VI)-transformed cells

Our previous study using RNAseq analysis showed that levels of genes associated with glycolysis, pentose phosphate pathway (PPP), and glutaminolysis were increased in Cr(VI)-transformed cells, while levels of genes associated with oxidative phosphorylation (OXPHOS) were reduced compared to those in passage-matched normal BEAS-2B cells (Clementino et al. 2018). In the present study, we performed a glycolytic stress analysis. The results showed that glycolysis (Figure 3.1A), glycolytic capacity (Figure 3.1B), and glycolytic reserve (Figure 3.1C) were all elevated in Cr(VI)-transformed cells compared to those in passage-matched normal BEAS-2B cells. Glycolysis is to measure extracellular acidification rate (ECAR) after the addition of saturating amounts of glucose. Glycolytic capacity is to measure the maximum ECAR rate reached after effectively shutting down oxidative phosphorylation, which drives glycolysis to its maximum capacity. Glycolytic reserve is to measure the ability of a cell to respond to energy demands. These three parameters reflect the ability of a cell to convert glucose into pyruvate, which produces ATP. Thus, our results indicate that glycolytic ATP production was increased in Cr(VI)-transformed cells.

To study enzymes involved in the elevated glycolysis, levels of hexokinase2 (HK2), phospho-fructo kinase 1 (PFK1) and 6-fosfofruto-2-quinase/frutose-2,6-bifosfatase 3 (PFKFB3), key glycolytic proteins, were examined. The results showed that all three proteins were upregulated in Cr(VI)-transformed cells compared to those in passage-matched normal BEAS-2B cells (Figure 3.1D).

3.4.2   Nrf2 overexpression increases glycolysis in normal BEAS-2B cells

The results from RNAseq analysis showed that Nrf2 overexpression in normal BEAS-2B cells caused increases of expressions of genes associated with

glycolysis and reduced expression of genes associated with OXPHOS (Supplementary Tables 1 and 2), indicating that Nrf2 may play an important role in metabolic reprogramming. The results from glycolytic stress test showed that forced overexpression of Nrf2 in BEAS-2B cells increased glycolysis, glycolytic capacity and glycolytic reserve (Figures 3.2A, 3.2B and 3.2C). Nrf2 overexpression also increased expression of glycolytic proteins including HK2, PFK1, and PFKFB3 (Figure 3.2D). Consistently, knockdown of Nrf2 by its shRNA reduced levels of HK2, PFK1 and PFKFB3 in Cr(VI)-transformed cells (Figure 3.2D). These results indicate that Nrf2 positively regulates glycolytic ATP generation in Cr(VI)-transformed cells.

Next, we investigated the mechanisms of increased glycolysis in Cr(VI)-transformed cells. The results from RNAseq analysis showed that overexpression of Nrf2 in normal BEAS-2B cells increased the expressions of genes associated with AMPK signaling pathway (Table 3.1). The genes of AMPKα regulatory subunit and activating AMPKα were upregulated, while the genes inhibiting AMPKα were downregulated in BEAS-2B cells with Nrf2 overexpression. Similar results were observed in Cr(VI)-transformed cells. Furthermore, glycolysis and lipid metabolism genes associated with AMPKα pathway were also upregulated in those Nrf2-expressing BEAS-2B cells and Cr(VI)-transformed cells.

Phosphorylation of AMPKα at threonine 172, a regulatory subunit of AMPKα, is required for AMPKα activation. Phosphorylation of AMPKα was increased in normal BEAS-2B cells with Nrf2 overexpression and in Cr(VI)-transformed cells (Figure 3.2E). Knockdown of Nrf2 by its shRNA in Cr(VI)-transformed cells reduced the AMPKα phosphorylation (Figure 3.2E). These results suggest that Nrf2 is a positive regulator of AMPKα activation in Cr(VI)-transformed cells, supporting the hypothesis that constitutive Nrf2 activation increases glycolysis in Cr(VI)-transformed cells via activation of AMPKα signaling pathway.

3.4.3 AMPKα inhibition reduces glycolysis in BEAS-2B cells with Nrf2 overexpression and Cr(VI)-transformed cells.

Next, we knockdown AMPKα by its shRNA in BEAS-2B cells with Nrf2 overexpression. Knockdown of AMPKα by its shRNA in Cr(VI)-transformed cells reduced protein levels of PFK1 and PFKFB3 (Figure 3.4A). Knockdown of AMPKα also reduced glycolysis, glycolytic capacity and glycolytic reserve in Cr(VI)-transformed cells (Figures 3.4B-D). These results suggest that AMPKα knockdown blocks activation of PFKFB3/PFK1 pathway, causing reduction of glycolytic ATP production.

Dorsomorphin is a potent and selective inhibitor of AMPKα (Choi et al. 2015; Zou et al. 2015). In Cr(VI)-transformed cells, treatment with dorsomorphin for 24h at concentrations of 1, 2, and 5 µM reduced protein levels of p-AMPKα^{Thr172}, PFK1, and PFKFB3 (Figure 3.5A). The results from glycolytic stress test showed that treatment with 5µM dorsomorphin significantly reduced glycolysis (Figure 3.5B), glycolytic capacity (Figure 3.5C) and glycolytic reserve (Figure 3.5D). These results suggest that activation of AMPKα regulates the glycolytic shift in Cr(VI)-transformed cells.

3.4.4 Constitutive Nrf2 activation leads to increased cell proliferation and tumorigenesis in Cr(VI)-transformed cells

We investigated whether constitutive Nrf2 activation is important for increased cell proliferation and tumorigenesis of Cr(VI)-transformed cells. Our results showed that knockdown of Nrf2 by its shRNA in Cr(VI)-transformed cells reduced cell proliferation on the days of 6 and 9, but not on the day 2 (Figure 3.6A). Nrf2 overexpression in normal BEAS-2B cells increased cell proliferation on days 6 and 9 (Figure 3.6A). The results from *in vivo* xenograft tumor growth assay showed in that 5 of 6 animals injected with Cr(VI)-transformed cells grew tumors (83%), and none of 6 animals injected with Cr(VI)-transformed cells with Nrf2 knockdown grew tumors (0%) (Figure 3.6B). None of the animals (out of 6)

injected with normal BEAS-2B cells grew tumors (0%), However, 4 out of 6 animals injected with BEAS-2B cells overexpressing Nrf2 grew tumors (67%) (Figure 3.6B). Both the tumor volume and weight in Cr(VI)-transformed cells are similar as those BEAS-2B cells with Nrf2 overexpression (Figures 3.6C and 3.6D). The results from immunoblotting analysis showed that in these tumor tissues levels of Nrf2, p-AMPKα^{Thr172}, AMPKα, HK2, PFK1, and PFKFB3 were detectable (Figures 3.6E and 3.6F). These results demonstrated that constitutive Nrf2 activation plays an important role in increased cell proliferation and tumorigenesis in Cr(VI)-transformed cells.

3.5   Discussion

In order to adapt to biological demands of increased proliferation, cancer cells change their metabolism by increasing glycolysis, PPP, and glutaminolysis (Hanahan and Weinberg). This metabolic shift was first described by Otto Warburg, known as the Warburg effect (Warburg 1956a; 1956b). Metabolic reprogramming is currently known as one of the hallmarks of cancer (Ward and Thompson 2012). Our previous (Clementino et al. 2018) and current studies showed that in Cr(VI)-transformed cells OXPHOS was downregulated and glycolysis, PPP and glutaminolysis pathways were upregulated, leading to reduced ATP production from OXPHOS and increased ATP from glycolysis. We observed that in Cr(VI)-transformed cells glycolysis was elevated. The extent of the increase in glycolysis may depend on the malignancy or aggressiveness of these transformed cells. Glycolysis might not change in Cr(VI)-transformed cells with less malignancy or aggressiveness. The Cr(VI)-transformed cells used in the present study are considered as aggressive ones as discussed in the Chapter 2. Our results demonstrated that Cr(VI)-transformed cells undergo metabolic reprogramming.

Nrf2 plays an important role in metabolic reprogramming by inhibiting lipogenesis, facilitating flux through PPP, inducing purine biosynthesis, regulating key metabolic proteins, and by cross-talking with several oncogenes (Chartoumpekis et al. 2015; Costa et al. 2014; Menegon et al. 2016; Panieri and Santoro 2016; Wende et al. 2016). Our results showed that in Cr(VI)-transformed cells, constitutive Nrf2 activation induces metabolic reprogramming, leading to increased cell proliferation and tumorigenesis of Cr(VI)-transformed cells. The present study has also demonstrated that overexpression of Nrf2 in normal BEAS-2B cells is tumorigenic.

HK2, PFK1, and PFKB3 are key proteins in regulation of glycolysis. These proteins regulate the first rate-limiting reactions of glycolysis. HK2 catabolizes the phosphorylation of glucose to glucose-6-phosphate (G6P) and PFK1 catabolizes the phosphorylation of fructose-6-phosphate (F6P). PFK1 is considered the

primary control point of glycolysis and it is often upregulated in cancer cells (Li et al. 2015). PFK1 activity is increased by fructose-2,6-biphosphate (F2,6BP), which is generated by phosphorylation of F6P through PFK2. In cancer cells, increased glucose uptake and high hexokinase activity increase F6P generation, thus yielding more F2,6BP, which in turn increases PFK1 activity (Alfarouk et al. 2014; Li et al. 2015). In Cr(VI)-transformed cells and normal BEAS-2B cells with Nrf2 overexpression, HK2, PFK1, and PFKB3 were all upregulated. Nrf2 knockdown in Cr(VI)-transformed cells reduced HK2, PFK1, and PFKB3 protein levels. The present study has demonstrated that glycolytic shift regulated by Nrf2 is through HK2, PFk1, and PFKB3 in Cr(VI)-transformed cells.

It has been reported that Nrf2 induced glycolytic shift in cancer is mediated by AMPKα activation (Wang et al. 2018). Our results showed that constitutive Nrf2 activation induces phosphorylation of AMPKα at threonine 172, a regulatory subunit of AMPK. This phosphorylation is required for AMPKα activation (Stein et al. 2000). Our results also showed that forced Nrf2 expression in normal cells increased p-AMPKα^{Thr172} level, while Nrf2 inhibition in Cr(VI)-transformed cells reduced it, suggesting that Nrf2 is a positive regulator of AMPKα. The results from RNAseq analysis showed that in cells with constitutively activated Nrf2 (normal BEA-2B cells with Nrf2 overexpression and Cr(VI)-transformed cells), expressions of genes associated with AMPK subunits and AMPKα activation were increased, however, expressions of genes associated with AMPKα inhibition were decreased. Our results also showed that expression of genes associated with glucose and lipid metabolism which are downstream of the AMPK signaling pathway were increased, demonstrating that AMPKα is activated in Cr(VI)-transformed cells. Rab, an oncogene, is known to induce glucose transporter type 4 (Glut4) translocation, which leads to increased glucose uptake. The increase in glucose uptake elevated hexokinases activity, resulting in the glycolytic shift through PFK1-PFK2 pathway (Brewer et al. 2016; Sano et al. 2007; Sano et al. 2008). Our results showed that expression of Rab10, a downstream target of AMPKα signaling pathway, was increased in

Cr(VI)-transformed cells, indicating that the role of AMPKα/Rab10 signal pathway in glycolytic shift of Cr(VI)-transformed cells.

In summary, our results demonstrated that constitutive Nrf2 activation activates AMPKα, leading to increased glycolysis, contributing to increased cell proliferation and tumorigenesis of Cr(VI)-transformed cells.
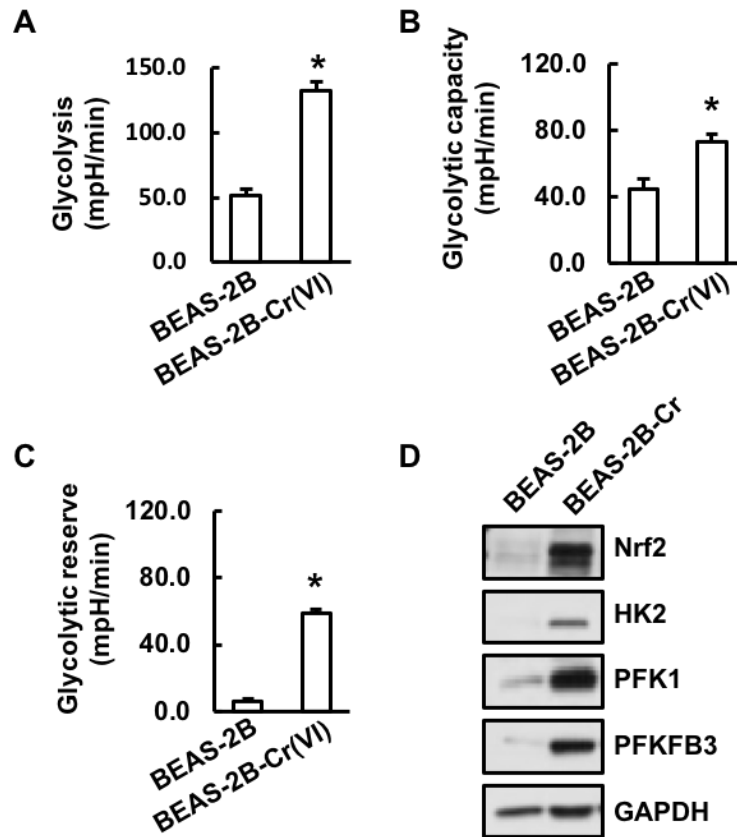
Figure 3.1 **Increased glycolysis in Cr(VI)-transformed cells**. (A), (B) and (C) Passage-matched normal BEAS-2B and Cr(VI)-transformed cells were seeded in 96-well plates for overnight. Glycolytic stress test was conducted using Seahorse analysis. Data are expressed as mean ± SD (n=8). *, $p < 0.05$, compared to those in passage-matched BEAS-2B cells. (D) Whole protein lysates from BEAS-2B cells and Cr(VI)-transformed cells were used for immunoblotting analysis.
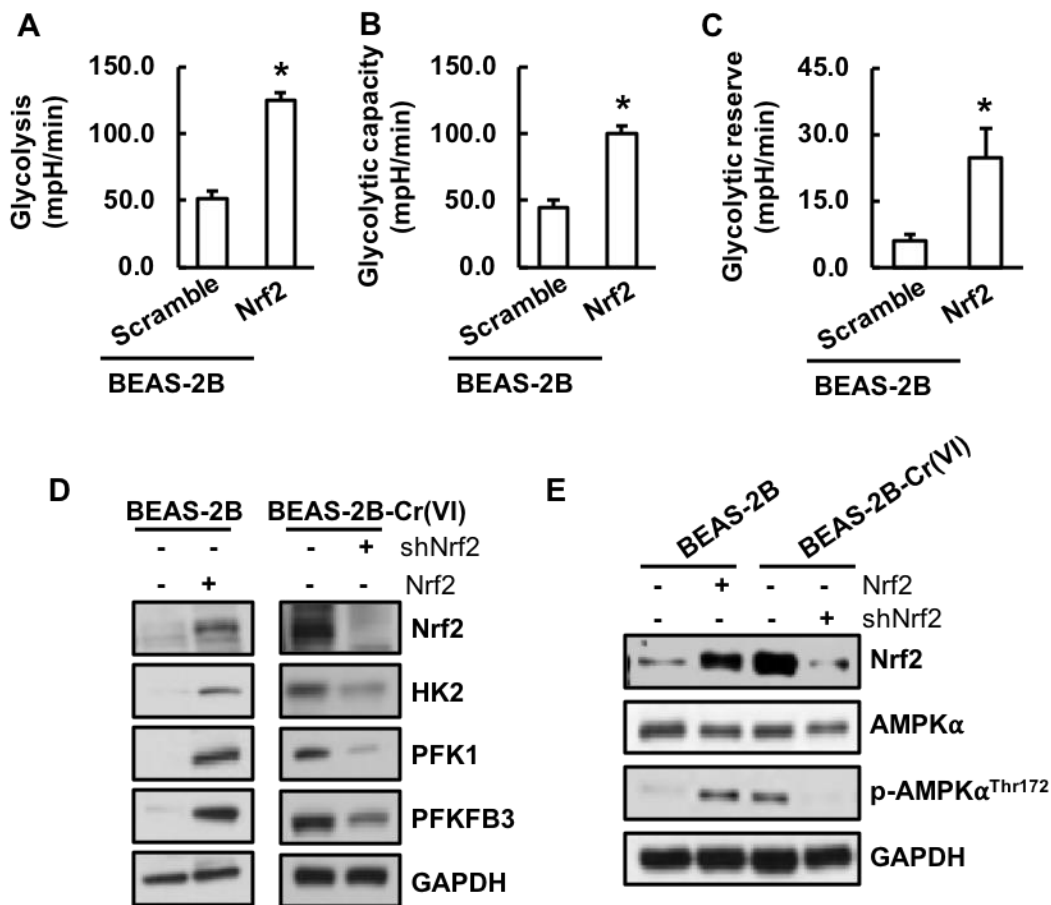
Figure 3.2 **Nrf2 overexpression in normal BEAS-2B cells increases glycolysis.** (A), (B) and (C) Normal BEAS-2B cells transfected with or without Nrf2 plasmid were seeded in 96-well plates for overnight. Glycolytic stress test was conducted using Seahorse analysis. Data are expressed as mean ± SD (n=8). *, $p < 0.05$, compared to those in scramble passage-matched BEAS-2B cells. (D) and (E) Whole cell lysates from normal BEAS-2B cells transfected with or without Nrf2 plasmid, and Cr(VI)-transformed cells transfected with or without shNrf2 were used for immunoblotting analysis.

Table 3.1 Relative level of AMPK signaling pathway in Cr(VI)-transformed cells and passage-matched normal cells transfected with scramble or Nrf2 vector

Gene Symbol	Function	BEAS-2B	BEAS-2B-Nrf2	BEAS-2B-Cr(VI)
PRKAG1	AMPK Subunit	9.9 ± 0.7	15.1 ± 4.4 *	18.6 ± 1.6 *
PRKAB2	AMPK Subunit	7.3 ± 0.9	9.0 ± 1.3 *	10.0 ± 3.6 *
PRKAA1	AMPK Subunit	29.2 ± 1.3	27.8 ± 2.4 *	21.1 ± 2.7 *
PRKAA2	AMPK Subunit	1.3 ± 0.1	2.3 ± 0.6 *	3.4 ± 1.0 *
EEF2K	Activates AMPK	6.3 ± 0.2	7.8 ± 0.6 * #	10 ± 0.6 *
CAMKK1	Activates AMPK	1.3 ± 1.8	8.5 ± 1.5 *	19.3 ± 2.5 *
ADIPOR1	Activates AMPK	1.5 ± 0.3	1.6 ± 1.2	3.1 ± 1.1 *
ADIPOR2	Activates AMPK	52.1 ± 3.8	47.9 ± 0.7 * #	41.9 ± 2.0 *
STK11	Inhibits AMPK	24.5 ± 2.5	19.6 ± 0.5 * #	13.8 ± 0.2 *
PPP2R5B	Inhibits AMPK	19.3 ± 1.3	13 ± 0.1 * #	1.1 ± 0.1 *
PPP2R5D	Inhibits AMPK	51.7 ± 5.0	38.4 ± 2.7 *	19.5 ± 3.8 *
PPP2CB	Inhibits AMPK	86.1 ± 8.3	78.8 ± 0.4 * #	59.3 ± 3.3 *
PPP2R3C	Inhibits AMPK	19.1 ± 1.8	15.3 ± 0.8 *	4.9 ± 1.8 *
PPP2R3B	Inhibits AMPK	8.8 ± 0.9	6.4 ± 0.6 * #	3.0 ± 1.3 *
PPP2R5E	Inhibits AMPK	7.8 ± 0.5	7.2 ± 0.6 * #	4.9 ± 0.7 *
STRADA	Inhibits AMPK	18.1 ± 0.2	14.8 ± 1.6 *	6.5 ± 1.7 *
CPT1C	Fatty acid metabolism	1.0 ± 1.1	2.0 ± 0.5 *	2.7 ± 0.2 *
MLYCD	Fatty acid metabolism	0.5 ± 0.1	0.9 ± 0.1 #	1.5 ± 0.1 *
ACACA	Fatty acid metabolism	0.2 ± 0.3	4.4 ± 1.4 * #	10.8 ± 1.5 *
SCD	Lipogenesis	14.9 ± 3.0	60.6 ± 5.6 *	143.3 ± 31.5 *
FASN	Lipogenesis	6.1 ± 2.4	14.1 ± 2.5 * #	24.7 ± 3.8
G6PC3	Glycolysis	29.0 ± 1.2	41.8 ± 3.9 *	64.0 ± 5.3 *
PFKM	Glycolysis	29.5 ± 4.7	46.3 ± 3.9 *	86.7 ± 2.9 *
SREBF1	Glucose/lipid metabolism	22.9 ± 1.5	26.4 ± 3.2 *	35.1 ± 10.2 *
RAB10	Oncogene	36.9 ± 3.6	55.2 ± 5.8 *	95.5 ± 24.9 *

Table 3.1 **Relative level of AMPK signaling pathway in Cr(VI)-transformed cells and passage-matched normal cells with or without Nrf2 expression**. Whole transcriptome sequencing analysis was performed using HiSeq 2500 Rapid Run.Differentially expressed genes involved in AMPK signalling pathway were detected using EBseq. Data are expressed as mean ± SD (n=3). * and #, p < 0.05, compared to those in scramble passage-matched BEAS-2B and Cr(VI)-transformed cells, respectively.
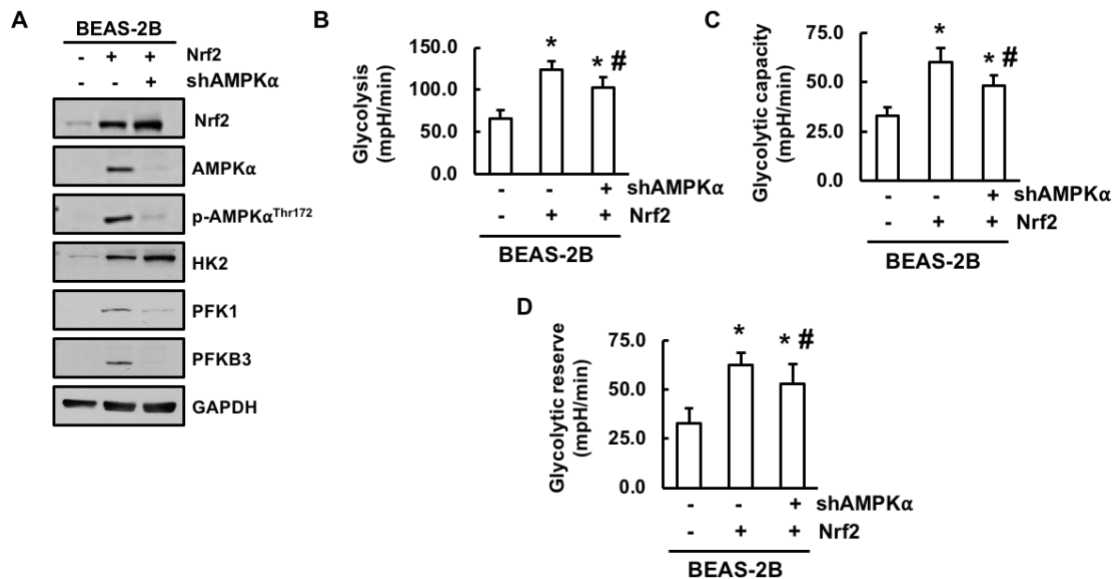
Figure 3.3 **AMPK inhibition reduces glycolysis in normal BEAS-2B cells with Nrf2 expression**. (A) Normal BEAS-2B cells were transfected with or without Nrf2 expression vector or together with AMPKα shRNA for 48 h. Whole protein lysates were harvested for immunoblotting analysis. (B), (C) and (D) Passage-matched normal BEAS-2B cells were transfected with or without Nrf2 expression vector, or together with AMPKα shRNA for 48 h. The cells were seeded in 96-well plates for overnight. Glycolytic stress test was conducted using Seahorse analysis. Data are expressed as mean ± SD (n=8). * and #, $p < 0.05$, compared to those in BEAS-2B cells transfected with scramble or Nrf2 vector, respectively.
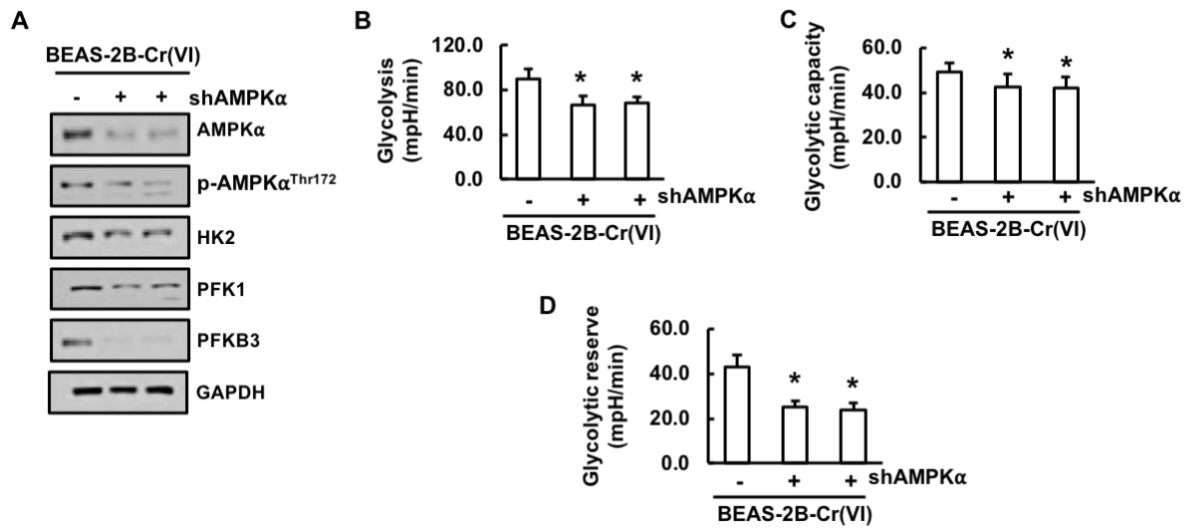
Figure 3.4 **AMPK inhibition reduces glycolysis in Cr(VI)-transformed cells**. (A) Cr(VI)-transformed cells were transfected with or without AMPKα shRNA for 48 h. Whole protein lysates were harvested for immunoblotting analysis. (B), (C) and (D) Cr(VI)-transformed cells transfected with or without AMPKα shRNA were seeded in 96-well plates for overnight. Glycolytic stress test was conducted using Seahorse analysis. Data are expressed as mean ± SD (n=8). *, $p < 0.05$, compared to those in Cr(VI)-transformed cells.
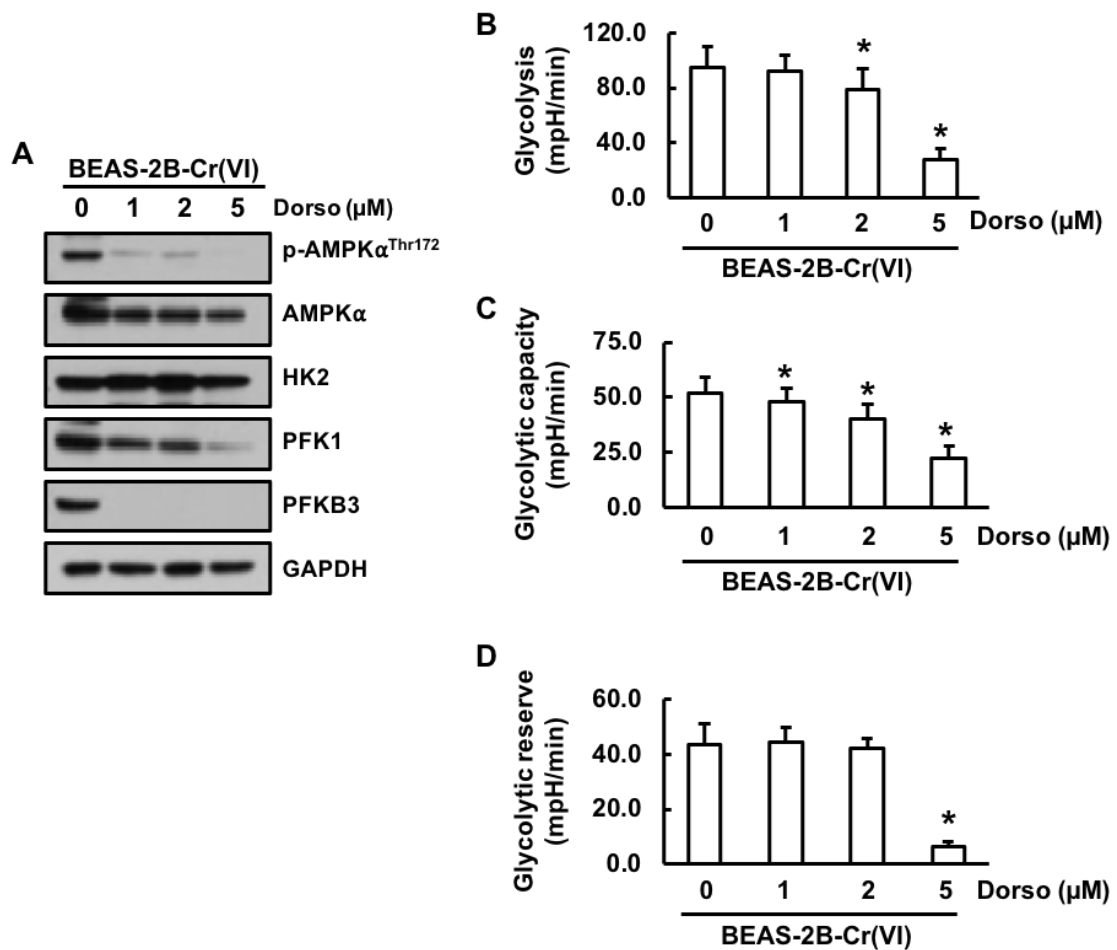
Figure 3.5 **Dorsomorphin treatment reduces AMPK activation and glycolysis in Cr(VI)-transformed cells.** (A) Cr(VI)-transformed cells were treated with 0, 1, 2, and 5 µM of Dorsomorphin for 24 h. Whole cell lysates were harvested for immunoblotting analysis. (B)-(D) Cr(VI)-transformed cells were treated with 0, 1, 2, and 5 µM of Dorsomorphin for 24 h. The cells were seeded in 96-well plates. Glycolytic stress was conducted using Seahorse analysis. Data are expressed as mean ± SD (n=8). *, $p <$ 0.05, compared to those in Cr(VI)-transformed cells without treatment.
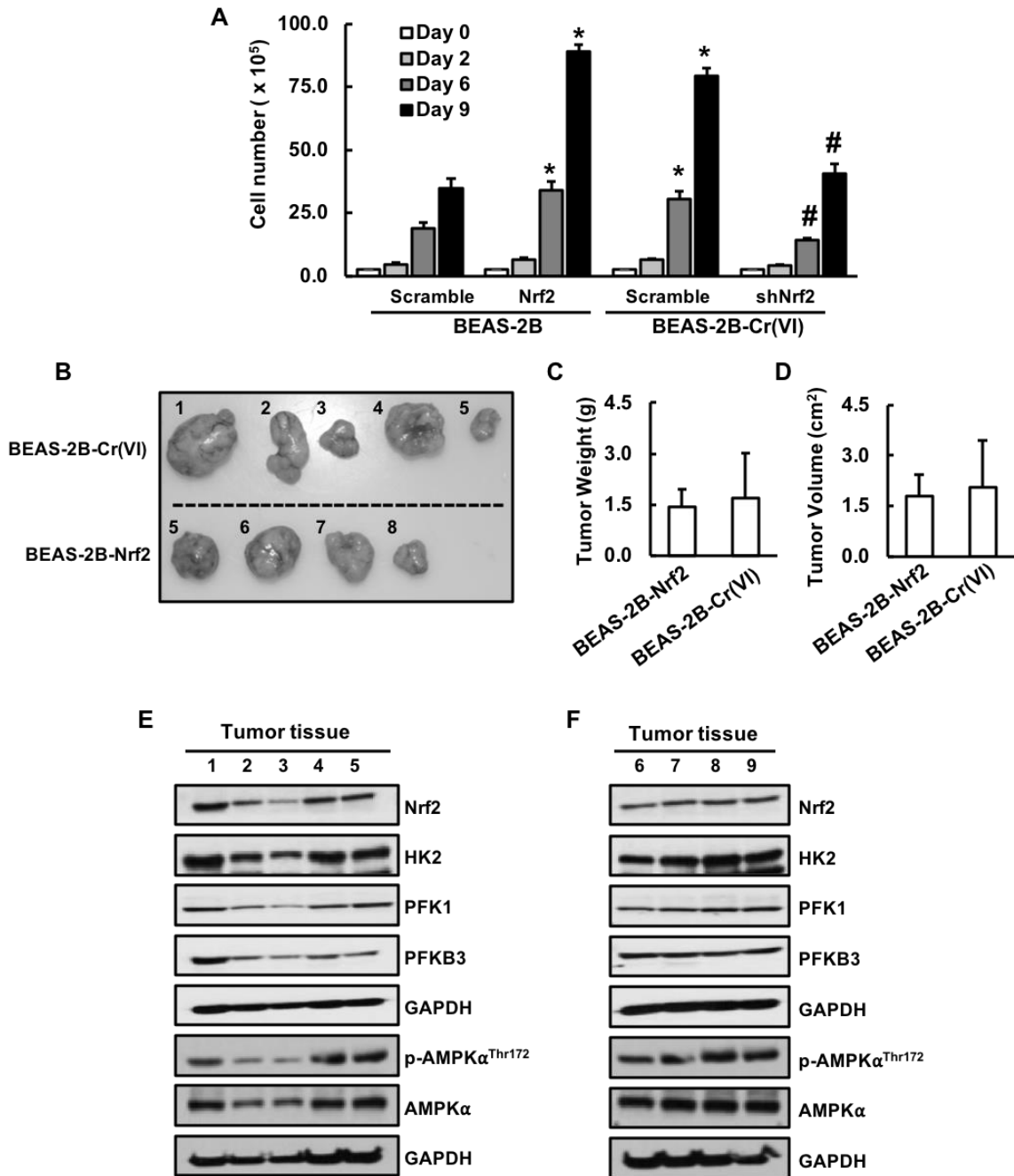
Figure 3.6 **Constitutive Nrf2 activation leads to increased cell proliferation and tumorigenesis of Cr(VI)-transformed cells.** (A) Passage-matched normal BEAS-2B cells with or without Nrf2 and Cr(VI)-transformed cells with or without Nrf2 shRNA were seeded in 6-well plates. The total cell number was counted at Day 0, 2, 6, and 9. Data are expressed as mean ± SD (n=8). * and #, $p < 0.05$ compared to that in same day BEAS-2B cells or Cr(VI)-transformed cells, respectively. (B), (C), and (D) 6-8 week old,

female immune-deficient mice were subcutaneously injected with normal BEAS-2B cells with or without Nrf2 expression or Cr(VI)-transformed cells with or without Nrf2 shRNA. After 3 weeks, the animals were euthanized using CO_2. The tumors were isolated and weighted (C) and pictures were captured (C). Tumor volumes (Length x Width^2/2) were measured (D). (C) and (D), data are expressed as mean ± SD (n=6). (E) and (F) Protein lysates were extracted from tumor tissues. Immunoblotting analysis was conducted to determine protein levels.

CHAPTER 4. CONCLUSIONS

4.1   Hexavalent Chromium in the Environment

Chromium compounds are naturally existed in earth's crust. Hexavalent chromium (Cr(VI)) is a toxic form of chromium. Cr(VI) is used in electroplating, wood preservatives, pigments, fungicides, and as ingredient and catalyst in chemical synthesis (Hausladen et al. 2018; United States. Occupational and Health 2009). Chromium is used to provide protective coatings to prevent corrosion; thus, the steel industry is a major consumer of chromium used in the production of stainless steel. (United States. Occupational and Health 2009). Workers exposed to Cr(VI) through inhalation may develop lung cancer, as well as irritation and/or damage to nose and lungs. Direct contact with skin and eyes caused irritation and/or damage to these organs (United States. Occupational and Health 2009). Workers inhale airborne Cr(VI) from dusts, fumes, and mists. Inhalation can occur while producing chromate pigments, powders and dyes; working near chromate electroplating; welding on stainless steel; and applying and removing chromate-containing paints. Skin and eyes exposure can occur while handling solution, coatings and cements containing Cr(VI).

Chromium is predominantly found in nature in two oxidation states, chromium (Cr(III)) and hexavalent chromium (Cr(VI)). Cr(VI) typically exists as chromate oxyanion, $H_xCrO_4^{x-2}$, which is a known carcinogen when exposure occurs via inhalation, and potentially carcinogenic when exposure happens via ingestion (Costa 1997; Sun et al. 2015; Welling et al. 2015). Chromate oxyanion is mobile in the environment; thus, it can contaminate water beds and jeopardize water quality. Industrial uses of chromium will lead to acute cases of groundwater Cr(VI)-contamination; however, oxidation of naturally occurring chromium by natural processes and anthropogenic activity may affect a larger area, more water beds, and more people (Hausladen et al. 2018). A recent study has analyzed the contribution of three primary Cr(VI) sources to pollute California's

ground water: Cr(VI) resulting from industrial pollution, injection of anthropogenic oxidants of naturally occurring Cr(III), and agricultural activities that may enhance oxidation of naturally occurring Cr(III) (Hausladen et al. 2018). Additionally, crops irrigation with untreated domestic and industrial effluents may result in accumulation of heavy metals in soils, leading to accumulation of Cr(VI) in the plant tissue (Stasinos and Zabetakis 2013).

4.2 Hexavalent Chromium Carcinogenesis

Metals are unique among pollutant toxicants because they are all naturally occurring and, in many cases, are already ubiquitous to some level within the human environment. Thus, regardless of how safely metals are used in industrial processes or consumer endpoint products, some level of human exposure is inevitable. Metals are neither created nor destroyed by human endeavors. Anthropogenic usage of metals increases the concentration of metals in the biosphere and alter their chemical speciation form, which thereby impact their toxicity potential. With a few very notable exceptions, most metals are only sparingly recycled once used. These factors combine altogether tend to make metals persistent in the human environment, often resulting in prolonged exposures. Cr(VI) is known to induce cancer in humans. It is classified as a Group1 human carcinogen by the International Agency for Research in Cancer (IARC). However, the mechanism by which Cr(VI) induces cancer is unknown.

Chronic exposure of normal bronchial epithelial (BEAS-2B) cells to low dose of Cr(VI) induces malignant cell transformation (Clementino et al. 2018; Dai et al. 2017; Kim et al. 2015a; Kim et al. 2016; Park et al. 2015; Pratheeshkumar et al. 2016; Zhang et al. 2015b). Once the cells are malignantly transformed, these cells exhibit reduced capacity of generating ROS, development of apoptosis resistance, induced angiogenesis, increased cell proliferation and tumorigenesis (Kim et al. 2016; Kim et al. 2015b; Lee et al. 2012; Pratheeshkumar et al. 2016; Wang et al. 2011).

69

Transformed cells adapt metabolism to support tumor initiation and progression. Altered metabolic activities directly participate in the process of cell transformation or support a large requirement for nucleotides, amino acids, and lipids for tumor growth. In malignantly Cr(VI)-transformed cells, mitochondrial oxidative phosphorylation is defective, pentose phosphate pathway, glycolysis, and glutaminolysis are upregulated. These metabolic reprogramming supports rapid cell proliferation and contributes to tumorigenesis of Cr(VI)-transformed cells. Chapter 1 summarized the current progress in the studies of metabolic reprogramming and Cr(VI) carcinogenesis with emphasis on the metabolic enzymes and oxidative stress related major oncogenic pathways.

The study in Chapter 2 investigated the role of NAD-dependent deacetylase Sirtuin-3 (SIRT3) in tumorigenesis of Cr(VI)-transformed cells. The results showed that In Cr(VI)-transformed cells, SIRT3 was upregulated and mitochondrial ATP production and proton leak were reduced. Inhibition of SIRT3 further decreased mitochondrial ATP production, proton leak and mitochondrial mass and increased mitochondrial membrane depolarization, indicating that SIRT3 positively regulates mitochondrial oxidative phosphorylation and maintenance of mitochondrial integrity. Mitophagy is critical to maintain proper cellular functions. In Cr(VI)-transformed cells expressions of Pink 1 and Parkin, two mitophagy proteins, were elevated, indicating that Cr(VI)-transformed cells are mitophagy deficient. Knockdown of SIRT3 induced mitophagy, suggesting that SIRT3 plays an important role in mitophagy deficiency of Cr(VI)-transformed cells. Our results also showed that in Cr(VI)-transformed cells binding of Nrf2 to ARE of SIRT3 gene promoter was dramatically increased. Inhibition of SIRT3 suppressed cell proliferation and tumorigenesis of Cr(VI)-transformed cells. This study demonstrated that upregulation of SIRT3 causes mitophagy deficiency, playing an important role in cell survival and tumorigenesis of Cr(VI)-transformed cells.

The study in Chapter 3 investigated the role of Nrf2 in regulating metabolic reprogramming in Cr(VI)-transformed cells. The results showed that Nrf2 is

constitutive activated in Cr(VI)-transformed cells. Cr(VI)-transformed cells exhibit reduced mitochondrial phosphorylation and increased glycolysis. Inhibition of Nrf2 in Cr(VI)-transformed cells increased mitochondrial phosphorylation and glycolysis. AMPK is a key protein to regulate glycolysis. Our results showed that AMPK is activated. Inhibition of AMPK reduced glycolysis of Cr(VI)-transformed cells. Further study suggested that Nrf2 is a positive regulator of AMPK/PFK1/PFK2 pathway. In summary, this study demonstrated that constitutive activation of Nrf2 play an important role in metabolic reprogramming, leading to increased cell proliferation and tumorigenesis of Cr(VI)-transformed cells.

Overall these studies demonstrated that Nrf2 is constitutively activated in Cr(VI)-transformed cells; that Nrf2 binds to ARE of SIRT3 promoter, causing upregulation of SIRT3, which in turn induced mitophagy deficiency, indicating importance of SIRT3 in maintenance of mitochondria mass and further in increased cell proliferation and tumorigenesis of Cr(VI)-transformed cells; and that Nrf2 is essential for metabolic reprogramming of Cr(VI)-transformed cells. Cr(VI)-transformed cells exhibit decreased oxidative phosphorylation and increased pentose phosphate pathway (PPP), glutaminolysis, and glycolysis. Nrf2 activates AMPKα, resulting in glycolytic shift in Cr(VI)-transformed cells. The role of Nrf2 in Cr(VI)-transformed cells metabolic reprogramming and mitochondria function is summarized in Figure 4.1.
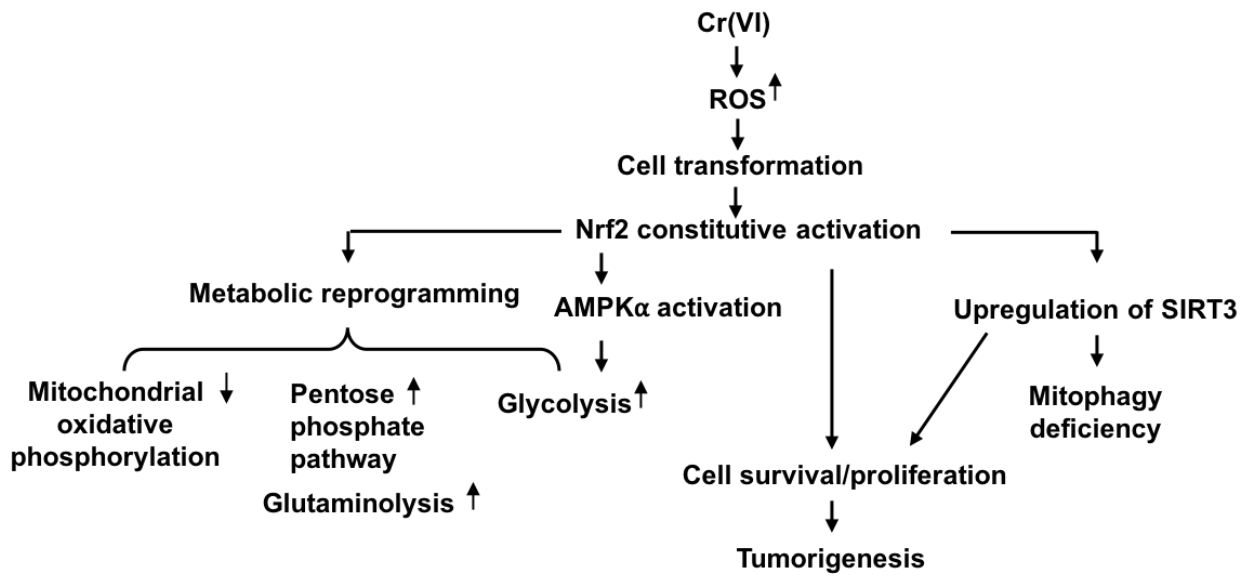
Figure 4.1 **The scheme of the role of Nrf2 in metabolic reprogramming and mitochondria function of Cr(VI)-transformed cells.** Chronic exposure of normal BEAS-2B cells to Hexavalent Chromium (Cr(VI)) at low dose induces malignant cell transformation. Nrf2 is upregulated in Cr(VI)-transformed cells. Nrf2 induces upregulation of SIRT3. SIRT3 expression leads to mitophagy deficiency, maintenance of mitochondria mass, increased cell proliferation and tumorigenesis in Cr(VI)-transformed cells. Additionally, Nrf2 expression leads to decreased oxidative phosphorylation, and increased glycolysis, pentose phosphate pathway and glutaminolisys in Cr(VI)-transformed cells. Nrf2 leads to the activation of AMPK signaling pathway, which contributes to the glycolytic shift observed in Cr(VI)-transformed cells. Futhermore, Nrf2 constitutive activation contributes to the rapid cell proliferation and tumorigenesis of Cr(VI)-transformed cells.
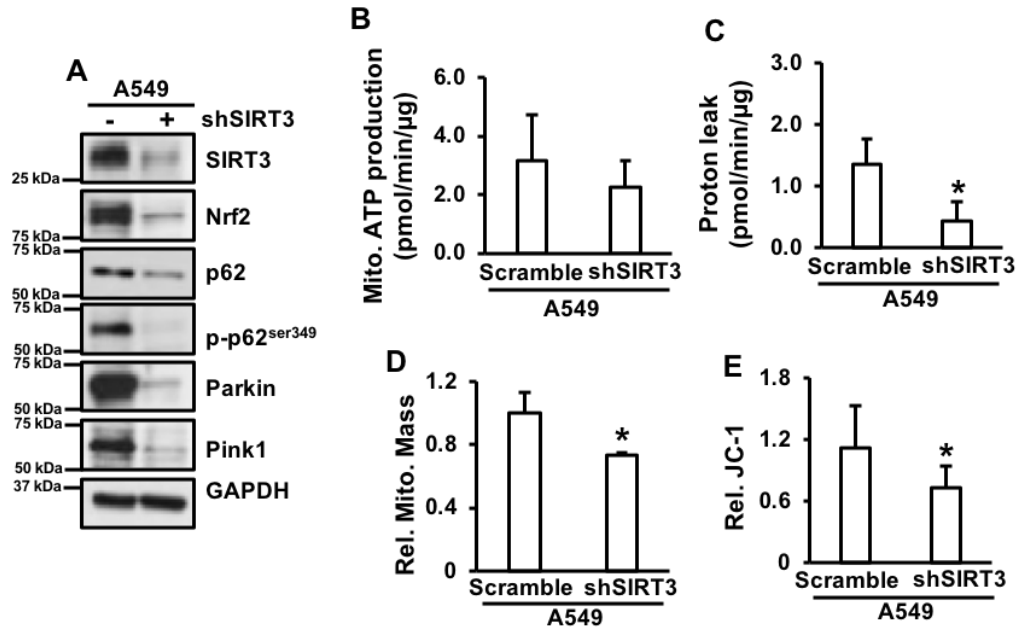
Supplemental Figure 1 **In A549 cells SIRT3 inhibition reduces p62 and Nrf2 protein levels, mitochondria mass, and mitochondrial oxidative phosphorylation function**. (A) Whole lysates from A549 cells were harvested for immunoblotting analysis. (B) and (C) A549 cells transfected with or without shSIRT3 were seeded in 96-well plates for overnight. Mitochondrial stress test was conducted using Seahorse analysis. (D) A549 cells transfected with or without shSIRT3 were seeded in 96-well plate for overnight. Mitochondrial mass was measured via NAO fluorescence intensity. (E) A549 cells transfected with shSIRT3 were seeded in 96-well plates for overnight. JC-1 fluorescence intensity was measured. Data are expressed as mean ± SD (n=8). *, $p < 0.05$, compared to that in scramble cells.

Supplementary Table 1 Relative level of metabolic enzymes in Cr(VI)-transformed cells and passage-matched normal cells with Nrf2 overexpression

Gene Symbol	Target pathway	BEAS-2B	BEAS-2B Nrf2	BEAS-2B-Cr(VI)
ADPGK	Glycolysis	0.4 ± 0.5	7.4 ± 0.6 *	6.7 ± 3.2 *
ALDOA	Glycolysis/PPP	6.8 ± 4.3	496.3 ± 14.2 * #	254.9 ± 57.0 *
DLAT	Glycolysis	14.7 ± 1.0	28.6 ± 1.5 * #	21.6 ± 2.6 *
ENO1	Glycolysis	1.5 ± 0.6	1.6 ± 1.2 #	71.6 ± 0.9 *
G6PC3	Glycolysis	50.7 ± 3.4	98.8 ± 6.7 *	97.3 ± 14.9 *
GPI	Glycolysis	19.1 ± 4.0	121.1 ± 11.2 * #	73.8 ± 8.9 *
HK2	Glycolysis	21.2 ± 3.8	36.1 ± 1.1 * #	32.1 ± 2.8 *
PDHA1	Glycolysis	48.9 ± 4.5	210.2 ± 11.3 * #	158.5 ± 11.7 *
PFKM	Glycolysis	29.5 ± 4.7	86.7 ± 3.9 * #	83.9 ± 3.6 *
PGK1	Glycolysis	107.5 ± 36.4	213.9 ± 26.6 * #	221.7 ± 68.5
PKM	Glycolysis	112.5 ± 70.6	65.3 ± 18.4 #	261 ± 73.9
G6PD	PPP	29.2 ± 5.3	222.0 ± 21.4 *	142.3 ± 50.2 *
PGD	PPP	6.8 ± 3.1	13.7 ± 0.8 * #	31.4 ± 5.9 *
PRPS1	PPP	59.4 ± 1.9	125.3 ± 4.0 * #	135.2 ± 8.1*
PRPS2	PPP	27.2 ± 0.1	74.6 ± 2.5 * #	53.6 ± 5.9
RPE	PPP	28.1 ± 1.7	42.6 ± 2.9 * #	39.0 ± 4.7 *
RPIA	PPP	20.1 ± 2.5	67.9 ± 0.4 * #	47.5 ± 2.7 *
TALDO1	PPP	28.8 ± 6.6	76.3 ± 8.0 * #	55.8 ± 7.7 *
TKT	PPP	151.9 ± 32.4	550.9 ± 36.0 * #	324.3 ± 85.5 *
GFPT1	Glutaminolysis	14.4 ± 1.4	20.5 ± 2.1 * #	26.8 ± 6.7 *
GLS	Glutaminolysis	19.3 ± 3.7	28.7 ± 2.8 *	30.3 ± 10.4

Supplementary Table 1 **Relative level of glycolysis, PPP and glutaminolysis transcripts in Cr(VI)-transformed cells and passage-matched normal cells transfected with scramble or Nrf2 vector.** Whole transcriptome sequencing analysis

was performed using HiSeq 2500 Rapid Run. Differentially expressed genes involved in AMPK signaling pathway were detected using EBseq. Data are expressed as mean ± SD (n=3). * and #, $p < 0.05$, compared to those in scramble passage-matched BEAS-2B, and Cr(VI)-transformed cells, respectively.

Supplementary Table 2 Relative level of enzymes involved in oxidative phosphorylation in Cr(VI)-transformed cells and passage-matched normal cells with Nrf2 overexpression

Gene Symbol	Mitochondrial complex	BEAS-2B	BEAS-2B Nrf2	BEAS-2B-Cr(VI)
NDUFA13	Complex I	58.1 ± 5.1	38.4 ± 1.1 *	34.9 ± 12.2 *
NDUFA11	Complex I	10.0 ± 0.2	5.6 ± 1.1 *	6.4 ± 1.0 *
NDUFC2	Complex I	154.6 ± 8.8	94.2 ± 5.5 *	87.3 ± 23.5 *
NDUFS8	Complex I	182.5 ± 2.0	137.6 ± 8.9 * #	99.2 ± 26.7 *
NDUFS7	Complex I	71.7 ± 3.1	75.8 ± 7.6 #	46.4 ± 13.4 *
NDUFS5	Complex I	544.2 ± 63.1	263.8 ± 15.1 *	271.8 ± 21.4 *
NDUFB7	Complex I	254.3 ± 16.4	161.1 ± 15.7 *	153.6 ± 29.6 *
NDUFV1	Complex I	12.5 ± 3.2	6.3 ± 2.2 *	5.8 ± 1.2 *
NDUFA6	Complex I	105.5 ± 2.8	0.0 ± 0.0 *	0.5 ± 0.8 *
NDUFA2	Complex I	152.4 ± 21.6	67.9 ± 2.6 *	72.6 ± 11.0 *
SDHA	Complex II	246.5 ± 37.5	128.2 ± 7.7 *	105.6 ± 20.1 *
UQCRC1	Complex III	108.1 ± 6.8	116.5 ± 9.7 #	84.5 ± 18.0
UQCR11	Complex III	160.3 ± 15.1	91.7 ± 11.2 *	101.5 ± 4.1 *
UQCR10	Complex III	103.6 ± 9.3	85.0 ± 7.1 * #	61.4 ± 9.1 *
UQCRH	Complex III	42.0 ± 3.1	23.1 ± 1.6 *	26.0 ± 2.1 *
COX4I1	Complex IV	8.3 ± 1.2	8.1 ± 1.7 #	3.4 ± 1.3 *
COX6A1	Complex IV	1.4 ± 0.5	1.4 ± 0.3 #	0.7 ± 0.1 *
COX6B1	Complex IV	4.7 ± 1.1	4.2 ± 0.2 #	2.5 ± 0.5 *
ATP5H	Complex V	631.8 ± 32.6	364.9 ± 14.5 *	362.8 ± 11.1 *
ATP5L	Complex V	119.5 ± 9.5	108.5 ± 8.2	87.3 ± 19.9 *
ATP5C1	Complex V	76.2 ± 15.7	2.6 ± 1.0 *	1.6 ± 0.6 *

Supplementary Table 2 **Relative level of Oxidative Phosphorylation transcripts in Cr(VI)-transformed cells and passage-matched normal cells transfected with scramble or Nrf2 vector.** Whole transcriptome sequencing analysis was performed using HiSeq 2500 Rapid Run. Differentially expressed genes involved in AMPK signaling pathway were detected using EBseq. Data are expressed as mean ± SD (n=3). * and #, $p < 0.05$, compared to those in scramble passage-matched BEAS-2B and Cr(VI)-transformed cells, respectively.

References

Ahn BH, Kim HS, Song S, Lee IH, Liu J, Vassilopoulos A, Deng CX, Finkel T. 2008. A role for the mitochondrial deacetylase sirt3 in regulating energy homeostasis. Proceedings of the National Academy of Sciences of the United States of America. 105(38):14447-14452.

Alfarouk KO, Verduzco D, Rauch C, Muddathir AK, Adil HHB, Elhassan GO, Ibrahim ME, David Polo Orozco J, Cardone RA, Reshkin SJ et al. 2014. Glycolysis, tumor metabolism, cancer growth and dissemination. A new ph-based etiopathogenic perspective and therapeutic approach to an old cancer question. Oncoscience. 1(12):777-802.

Barchowsky A, Klei LR, Dudek EJ, Swartz HM, James PE. 1999. Stimulation of reactive oxygen, but not reactive nitrogen species, in vascular endothelial cells exposed to low levels of arsenite. Free Radical Biology & Medicine. 27(11-12):1405-1412.

Bell EL, Guarente L. 2011. The sirt3 divining rod points to oxidative stress. Molecular Cell. 42(5):561-568.

Bensinger SJ, Christofk HR. 2012. New aspects of the warburg effect in cancer cell biology. Seminars In Cell & Developmental Biology. 23(4):352-361.

Bernardini JP, Lazarou M, Dewson G. 2017. Parkin and mitophagy in cancer. Oncogene. 36(10):1315-1327.

Bertout JA, Patel SA, Simon MC. 2008. The impact of o2 availability on human cancer. Nature Reviews Cancer. 8(12):967-975.

Birner P, Schindl M, Obermair A, Plank C, Breitenecker G, Oberhuber G. 2000. Overexpression of hypoxia-inducible factor 1alpha is a marker for an unfavorable prognosis in early-stage invasive cervical cancer. Cancer Research. 60(17):4693-4696.

Blancher C, Moore JW, Talks KL, Houlbrook S, Harris AL. 2000. Relationship of hypoxia-inducible factor (hif)-1alpha and hif-2alpha expression to vascular endothelial growth factor induction and hypoxia survival in human breast cancer cell lines. Cancer Research. 60(24):7106-7113.

Brewer PD, Habtemichael EN, Romenskaia I, Mastick CC, Coster ACF. 2016. Glut4 is sorted from a rab10 gtpase-independent constitutive recycling pathway into a highly insulin-responsive rab10 gtpase-dependent sequestration pathway after adipocyte differentiation. The Journal Of Biological Chemistry. 291(2):773-789.

Chan K, Han XD, Kan YW. 2001. An important function of nrf2 in combating oxidative stress: Detoxification of acetaminophen. Proceedings of the National Academy of Sciences of the United States of America. 98(8):4611-4616.

Chartoumpekis Dionysios V, Wakabayashi N, Kensler Thomas W. 2015. Keap1/nrf2 pathway in the frontiers of cancer and non-cancer cell metabolism. Biochemical Society Transactions. 43(4):639-644.

Chen M, Zhang J, Li N, Qian Z, Zhu M, Li Q, Zheng J, Wang X, Shi G. 2011. Promoter hypermethylation mediated downregulation of fbp1 in human hepatocellular carcinoma and colon cancer. Plos One. 6(10):e25564.

Chen Y, Fu LL, Wen X, Wang XY, Liu J, Cheng Y, Huang J. 2014. Sirtuin-3 (sirt3), a therapeutic target with oncogenic and tumor-suppressive function in cancer. Cell Death & Disease. 5(2):e1047.

Choi HS, Jeon HJ, Lee OH, Lee BY. 2015. Dieckol, a major phlorotannin in ecklonia cava, suppresses lipid accumulation in the adipocytes of high-fat diet-fed zebrafish and mice: Inhibition of early adipogenesis via cell-cycle arrest and ampkalpha activation. Molecular Nutrition & Food Research. 59(8):1458-1471.

Chourasia AH, Boland ML, Macleod KF. 2015. Mitophagy and cancer. Cancer & Metabolism. 3:4.

Cimen H, Han MJ, Yang Y, Tong Q, Koc H, Koc EC. 2010. Regulation of succinate dehydrogenase activity by sirt3 in mammalian mitochondria. Biochemistry. 49(2):304-311.

Clementino M, Shi X, Zhang Z. 2018. Oxidative stress and metabolic reprogramming in cr(vi) carcinogenesis. Current Opinion in Toxicology. 8:20-27.

Costa A, Scholer-Dahirel A, Mechta-Grigoriou F. 2014. The role of reactive oxygen species and metabolism on cancer cells and their microenvironment. Seminars in Cancer Biology. 25:23-32.

Costa M. 1997. Toxicity and carcinogenicity of cr(vi) in animal models and humans. Critical Reviews In Toxicology. 27(5):431-442.

Dai J, Ji Y, Wang W, Kim D, Fai LY, Wang L, Luo J, Zhang Z. 2017. Loss of fructose-1,6-bisphosphatase induces glycolysis and promotes apoptosis resistance of cancer stem-like cells: An important role in hexavalent chromium-induced carcinogenesis. Toxicology and Applied Pharmacology. 331:164-173.

Dang CV. 2010. Glutaminolysis: Supplying carbon or nitrogen or both for cancer cells? Cell Cycle (Georgetown, Tex). 9(19):3884-3886.

Dang CV, Kim JW, Gao P, Yustein J. 2008. The interplay between myc and hif in cancer. Nature Reviews Cancer. 8(1):51-56.

Das S, Mitrovsky G, Vasanthi HR, Das DK. 2014. Antiaging properties of a grape-derived antioxidant are regulated by mitochondrial balance of fusion and fission leading to mitophagy triggered by a signaling network of sirt1-sirt3-foxo3-pink1-parkin. Oxidative Medicine and Cellular Longevity. 2014:345105.

Daye D, Wellen KE. 2012. Metabolic reprogramming in cancer: Unraveling the role of glutamine in tumorigenesis. Seminars in Cell & Developmental Biology. 23(4):362-369.

DeBerardinis RJ, Cheng T. 2010. Q's next: The diverse functions of glutamine in metabolism, cell biology and cancer. Oncogene. 29(3):313-324.

Deberardinis RJ, Sayed N, Ditsworth D, Thompson CB. 2008. Brick by brick: Metabolism and tumor cell growth. Current Opinion in Genetics & Development. 18(1):54-61.

DeNicola GM, Chen PH, Mullarky E, Sudderth JA, Hu Z, Wu D, Tang H, Xie Y, Asara JM, Huffman KE et al. 2015. Nrf2 regulates serine biosynthesis in non-small cell lung cancer. Nature Genetics. 47(12):1475-1481.

Ding WX, Yin XM. 2012. Mitophagy: Mechanisms, pathophysiological roles, and analysis. Biological Chemistry. 393(7):547-564.

Dinkova-Kostova AT, Abramov AY. 2015. The emerging role of nrf2 in mitochondrial function. Free Radical Biology & Medicine.

Dong BW, Qin GM, Luo Y, Mao JS. 2017. Metabolic enzymes: Key modulators of functionality in cancer stem-like cells. Oncotarget. 8(8):14251-14267.

Dong C, Yuan T, Wu Y, Wang Y, Fan TW, Miriyala S, Lin Y, Yao J, Shi J, Kang T et al. 2013. Loss of fbp1 by snail-mediated repression provides metabolic advantages in basal-like breast cancer. Cancer Cell. 23(3):316-331.

Durcan TM, Fon EA. 2015. The three 'p's of mitophagy: Parkin, pink1, and post-translational modifications. Genes & Development. 29(10):989-999.

Eiyama A, Okamoto K. 2015. Pink1/parkin-mediated mitophagy in mammalian cells. Current Opinion in Cell Biology. 33:95-101.

Elstrom RL, Bauer DE, Buzzai M, Karnauskas R, Harris MH, Plas DR, Zhuang H, Cinalli RM, Alavi A, Rudin CM et al. 2004. Akt stimulates aerobic glycolysis in cancer cells. Cancer Research. 64(11):3892-3899.

Fan J, Kamphorst JJ, Mathew R, Chung MK, White E, Shlomi T, Rabinowitz JD. 2013. Glutamine-driven oxidative phosphorylation is a major atp source in transformed mammalian cells in both normoxia and hypoxia. Molecular Systems Biology. 9:712.

Ferlini C, Scambia G. 2007. Assay for apoptosis using the mitochondrial probes, rhodamine123 and 10-n-nonyl acridine orange. Nature Protocols. 2(12):3111-3114.

Finley LW, Haas W, Desquiret-Dumas V, Wallace DC, Procaccio V, Gygi SP, Haigis MC. 2011. Succinate dehydrogenase is a direct target of sirtuin 3 deacetylase activity. Plos One. 6(8):e23295.

Finley LW, Haigis MC. 2012. Metabolic regulation by sirt3: Implications for tumorigenesis. Trends in Molecular Medicine. 18(9):516-523.

Geisler S, Holmstrom KM, Skujat D, Fiesel FC, Rothfuss OC, Kahle PJ, Springer W. 2010. Pink1/parkin-mediated mitophagy is dependent on vdac1 and p62/sqstm1. Nature Cell Biology. 12(2):119-131.

Giatromanolaki A, Koukourakis MI, Sivridis E, Turley H, Talks K, Pezzella F, Gatter KC, Harris AL. 2001. Relation of hypoxia inducible factor 1 alpha and 2 alpha in operable non-small cell lung cancer to angiogenic/molecular profile of tumours and survival. British Journal of Cancer. 85(6):881-890.

Giralt A, Villarroya F. 2012. Sirt3, a pivotal actor in mitochondrial functions: Metabolism, cell death and aging. The Biochemical journal. 444(1):1-10.

Hanahan D, Weinberg Robert A. 2011. Hallmarks of cancer: The next generation. Cell. 144(5):646-674.

Harris GK, Shi X. 2003. Signaling by carcinogenic metals and metal-induced reactive oxygen species. Mutation Research. 533(1-2):183-200.

Hartmannsberger D, Mack B, Eggert C, Denzel S, Stepp H, Betz CS, Gires O. 2011. Transketolase-like protein 1 confers resistance to serum withdrawal in vitro. Cancer Letters. 300(1):20-29.

Hausladen DM, Alexander-Ozinskas A, McClain C, Fendorf S. 2018. Hexavalent chromium sources and distribution in california groundwater. Environmental Science & Technology. 52(15):8242-8251.

Hawkins KE, Joy S, Delhove JM, Kotiadis VN, Fernandez E, Fitzpatrick LM, Whiteford JR, King PJ, Bolanos JP, Duchen MR et al. 2016. Nrf2 orchestrates the metabolic shift during induced pluripotent stem cell reprogramming. Cell Reports. 14(8):1883-1891.

Hayes JD, McMahon M, Chowdhry S, Dinkova-Kostova AT. 2010. Cancer chemoprevention mechanisms mediated through the keap1-nrf2 pathway. Antioxidants & Redox Signaling. 13(11):1713-1748.

He ZL, Yang XE, Stoffella PJ. 2005. Trace elements in agroecosystems and impacts on the environment. Journal of Trace Elements in Medicine and Biology : Organ of the Society for Minerals and Trace Elements (GMS). 19(2-3):125-140.

Heiss EH, Schachner D, Zimmermann K, Dirsch VM. 2013. Glucose availability is a decisive factor for nrf2-mediated gene expression. Redox Biology. 1:359-365.

Holmström KM, Kostov RV, Dinkova-Kostova AT. 2017. The multifaceted role of nrf2 in mitochondrial function. Current Opinion in Toxicology. 2:80-91.

Hu R, Saw CL-L, Yu R, Kong A-NT. 2010. Regulation of nf-e2-related factor 2 signaling for cancer chemoprevention: Antioxidant coupled with antiinflammatory. Antioxidants & Redox Signaling. 13(11):1679-1698.

Huang LE, Arany Z, Livingston DM, Bunn HF. 1996. Activation of hypoxia-inducible transcription factor depends primarily upon redox-sensitive stabilization of its alpha subunit. The Journal of Biological Chemistry. 271(50):32253-32259.

Huss WJ, Hanrahan CF, Barrios RJ, Simons JW, Greenberg NM. 2001. Angiogenesis and prostate cancer: Identification of a molecular progression switch. Cancer Research. 61(6):2736-2743.

Ichimura Y, Waguri S, Sou Y-s, Kageyama S, Hasegawa J, Ishimura R, Saito T, Yang Y, Kouno T, Fukutomi T et al. Phosphorylation of p62 activates the keap1-nrf2 pathway during selective autophagy. Molecular Cell. 51(5):618-631.

Ivankovic D, Chau KY, Schapira AH, Gegg ME. 2016. Mitochondrial and lysosomal biogenesis are activated following pink1/parkin-mediated mitophagy. Journal of Neurochemistry. 136(2):388-402.

Jain A, Lamark T, Sjottem E, Larsen KB, Awuh JA, Overvatn A, McMahon M, Hayes JD, Johansen T. 2010. P62/sqstm1 is a target gene for transcription factor nrf2 and creates a positive feedback loop by inducing antioxidant response element-driven gene transcription. The Journal of Biological Chemistry. 285(29):22576-22591.

Jonas SK, Benedetto C, Flatman A, Hammond RH, Micheletti L, Riley C, Riley PA, Spargo DJ, Zonca M, Slater TF. 1992. Increased activity of 6-phosphogluconate dehydrogenase and glucose-6-phosphate dehydrogenase in purified cell suspensions and single cells from the

uterine cervix in cervical intraepithelial neoplasia. British Journal of Cancer. 66(1):185-191.

Kaczmarek M, Timofeeva OA, Karaczyn A, Malyguine A, Kasprzak KS, Salnikow K. 2007. The role of ascorbate in the modulation of hif-1alpha protein and hif-dependent transcription by chromium(vi) and nickel(ii). Free Radical Biology & Medicine. 42(8):1246-1257.

Kallio PJ, Wilson WJ, O'Brien S, Makino Y, Poellinger L. 1999. Regulation of the hypoxia-inducible transcription factor 1alpha by the ubiquitin-proteasome pathway. The Journal of Biological Chemistry. 274(10):6519-6525.

Kansanen E, Kuosmanen SM, Leinonen H, Levonen A-L. 2013a. The keap1-nrf2 pathway: Mechanisms of activation and dysregulation in cancer. Redox Biology. 1(1):45-49.

Kansanen E, Kuosmanen SM, Leinonen H, Levonen AL. 2013b. The keap1-nrf2 pathway: Mechanisms of activation and dysregulation in cancer. Redox Biology. 1:45-49.

Katsuragi Y, Ichimura Y, Komatsu M. 2016a. Regulation of the keap1–nrf2 pathway by p62/sqstm1. Current Opinion in Toxicology. 1(Supplement C):54-61.

Katsuragi Y, Ichimura Y, Komatsu M. 2016b. Regulation of the keap1–nrf2 pathway by p62/sqstm1. Current Opinion in Toxicology. 1:54-61.

Kim D, Dai J, Fai LY, Yao H, Son YO, Wang L, Pratheeshkumar P, Kondo K, Shi X, Zhang Z. 2015a. Constitutive activation of epidermal growth factor receptor promotes tumorigenesis of cr(vi)-transformed cells through decreased reactive oxygen species and apoptosis resistance development. The Journal of Biological Chemistry. 290(4):2213-2224.

Kim D, Dai J, Park YH, Fai LY, Wang L, Pratheeshkumar P, Son YO, Kondo K, Xu M, Luo J et al. 2016. Activation of epidermal growth factor receptor/p38/hypoxia-inducible factor-1alpha is pivotal for angiogenesis and tumorigenesis of malignantly transformed cells induced by hexavalent chromium. The Journal of Biological Chemistry. 291(31):16271-16281.

Kim HS, Kim YJ, Seo YR. 2015b. An overview of carcinogenic heavy metal: Molecular toxicity mechanism and prevention. Journal of Cancer Prevention. 20(4):232-240.

Kim JW, Tchernyshyov I, Semenza GL, Dang CV. 2006. Hif-1-mediated expression of pyruvate dehydrogenase kinase: A metabolic switch required for cellular adaptation to hypoxia. Cell Metabolism. 3(3):177-185.

Kobayashi M, Yamamoto M. 2006. Nrf2-keap1 regulation of cellular defense mechanisms against electrophiles and reactive oxygen species. Advances in Enzyme Regulation. 46:113-140.

Koutras GA, Hattori M, Schneider AS, Ebaugh FG, Jr., Valentine WN. 1964. Studies on chromated erythrocytes. Effect of sodium chromate on erythrocyte glutathione reductase. The Journal of Clinical Investigation. 43:323-331.

Kuleshov MV, Jones MR, Rouillard AD, Fernandez NF, Duan Q, Wang Z, Koplev S, Jenkins SL, Jagodnik KM, Lachmann A et al. 2016. Enrichr: A

comprehensive gene set enrichment analysis web server 2016 update. Nucleic Acids Research. 44(Web Server issue):W90-W97.

Kulikov AV, Luchkina EA, Gogvadze V, Zhivotovsky B. 2017. Mitophagy: Link to cancer development and therapy. Biochemical and Biophysical Research Communications. 482(3):432-439.

Langard S. 1990. One hundred years of chromium and cancer: A review of epidemiological evidence and selected case reports. American Journal of Industrial Medicine. 17(2):189-215.

Langard S. 1993. Role of chemical species and exposure characteristics in cancer among persons occupationally exposed to chromium compounds. Scandinavian Journal of Work, Environment & Health. 19 Suppl 1:81-89.

Lau A, Whitman SA, Jaramillo MC, Zhang DD. 2013. Arsenic-mediated activation of the nrf2-keap1 antioxidant pathway. Journal of Biochemical and Molecular Toxicology. 27(2):99-105.

Lazarou M, Sliter DA, Kane LA, Sarraf SA, Wang C, Burman JL, Sideris DP, Fogel AI, Youle RJ. 2015. The ubiquitin kinase pink1 recruits autophagy receptors to induce mitophagy. Nature. 524(7565):309-314.

Lee CH, Yu HS. 2016. Role of mitochondria, ros, and DNA damage in arsenic induced carcinogenesis. Frontiers in Bioscience (Scholar edition). 8:312-320.

Lee HC, Yin PH, Lu CY, Chi CW, Wei YH. 2000. Increase of mitochondria and mitochondrial DNA in response to oxidative stress in human cells. The Biochemical Journal. 348(Pt 2):425-432.

Lee JC, Son YO, Pratheeshkumar P, Shi X. 2012. Oxidative stress and metal carcinogenesis. Free Radical Biology & Medicine. 53(4):742-757.

Leng N, Li Y, McIntosh BE, Nguyen BK, Duffin B, Tian S, Thomson JA, Dewey CN, Stewart R, Kendziorski C. 2015. Ebseq-hmm: A bayesian approach for identifying gene-expression changes in ordered rna-seq experiments. Bioinformatics (Oxford, England). 31(16):2614-2622.

Li B, Dewey CN. 2011. Rsem: Accurate transcript quantification from rna-seq data with or without a reference genome. BMC Bioinformatics. 12:323.

Li B, Qiu B, Lee DS, Walton ZE, Ochocki JD, Mathew LK, Mancuso A, Gade TP, Keith B, Nissim I et al. 2014. Fructose-1,6-bisphosphatase opposes renal carcinoma progression. Nature. 513(7517):251-255.

Li X-b, Gu J-d, Zhou Q-h. 2015. Review of aerobic glycolysis and its key enzymes – new targets for lung cancer therapy. Thoracic Cancer. 6(1):17-24.

Liang Q, Benavides GA, Vassilopoulos A, Gius D, Darley-Usmar V, Zhang J. 2013. Bioenergetic and autophagic control by sirt3 in response to nutrient deprivation in mouse embryonic fibroblasts. The Biochemical Journal. 454(2):249-257.

Liu R, Fan M, Candas D, Qin L, Zhang X, Eldridge A, Zou JX, Zhang T, Juma S, Jin C et al. 2015. Cdk1-mediated sirt3 activation enhances mitochondrial function and tumor radioresistance. Molecular Cancer Therapeutics. 14(9):2090-2102.

Liu SX, Athar M, Lippai I, Waldren C, Hei TK. 2001. Induction of oxyradicals by arsenic: Implication for mechanism of genotoxicity. Proceedings of the National Academy of Sciences of the United States of America. 98(4):1643-1648.

Lombard DB, Alt FW, Cheng HL, Bunkenborg J, Streeper RS, Mostoslavsky R, Kim J, Yancopoulos G, Valenzuela D, Murphy A et al. 2007. Mammalian sir2 homolog sirt3 regulates global mitochondrial lysine acetylation. Molecular and Cellular Biology. 27(24):8807-8814.

Lu J, Tan M, Cai Q. 2015. The warburg effect in tumor progression: Mitochondrial oxidative metabolism as an anti-metastasis mechanism. Cancer Letters. 356(2 Pt A):156-164.

Machle W, Gregorius F. 1948. Cancer of the respiratory system in the united states chromate producing industry. Public Health Reports (Washington, DC : 1896). 63(35):1114-1127.

Maftah A, Petit JM, Ratinaud MH, Julien R. 1989. 10-n nonyl-acridine orange: A fluorescent probe which stains mitochondria independently of their energetic state. Biochemical and Biophysical Research Communications. 164(1):185-190.

Majumder PK, Febbo PG, Bikoff R, Berger R, Xue Q, McMahon LM, Manola J, Brugarolas J, McDonnell TJ, Golub TR et al. 2004. Mtor inhibition reverses akt-dependent prostate intraepithelial neoplasia through regulation of apoptotic and hif-1-dependent pathways. Nature Medicine. 10(6):594-601.

Maxwell PH, Dachs GU, Gleadle JM, Nicholls LG, Harris AL, Stratford IJ, Hankinson O, Pugh CW, Ratcliffe PJ. 1997. Hypoxia-inducible factor-1 modulates gene expression in solid tumors and influences both angiogenesis and tumor growth. Proceedings of the National Academy of Sciences of the United States of America. 94(15):8104-8109.

Menegon S, Columbano A, Giordano S. 2016. The dual roles of nrf2 in cancer. Trends in Molecular Medicine. 22(7):578-593.

Mitsuishi Y, Taguchi K, Kawatani Y, Shibata T, Nukiwa T, Aburatani H, Yamamoto M, Motohashi H. 2012. Nrf2 redirects glucose and glutamine into anabolic pathways in metabolic reprogramming. Cancer Cell. 22(1):66-79.

Morris KC, Lin HW, Thompson JW, Perez-Pinzon MA. 2011. Pathways for ischemic cytoprotection: Role of sirtuins in caloric restriction, resveratrol, and ischemic preconditioning. Journal of Cerebral Blood Flow and Metabolism : Official Journal of the International Society of Cerebral Blood Flow and Metabolism. 31(4):1003-1019.

Ni H-M, Williams JA, Ding W-X. 2015. Mitochondrial dynamics and mitochondrial quality control. Redox Biology. 4:6-13.

Niture SK, Kaspar JW, Shen J, Jaiswal AK. 2010. Nrf2 signaling and cell survival. Toxicology and Applied Pharmacology. 244(1):37-42.

Ohta T, Iijima K, Miyamoto M, Nakahara I, Tanaka H, Ohtsuji M, Suzuki T, Kobayashi A, Yokota J, Sakiyama T et al. 2008. Loss of keap1 function activates nrf2 and provides advantages for lung cancer cell growth. Cancer Research. 68(5):1303-1309.

Panieri E, Santoro MM. 2016. Ros homeostasis and metabolism: A dangerous liason in cancer cells. Cell Death Dis. 7(6):e2253.

Papandreou I, Cairns RA, Fontana L, Lim AL, Denko NC. 2006. Hif-1 mediates adaptation to hypoxia by actively downregulating mitochondrial oxygen consumption. Cell Metabolism. 3(3):187-197.

Park SH, Ozden O, Jiang H, Cha YI, Pennington JD, Aykin-Burns N, Spitz DR, Gius D, Kim HS. 2011. Sirt3, mitochondrial ros, ageing, and carcinogenesis. International Journal of Molecular Sciences. 12(9):6226-6239.

Park YH, Kim D, Dai J, Zhang Z. 2015. Human bronchial epithelial beas-2b cells, an appropriate in vitro model to study heavy metals induced carcinogenesis. Toxicology and Applied Pharmacology. 287(3):240-245.

Pellegrini L, Pucci B, Villanova L, Marino ML, Marfe G, Sansone L, Vernucci E, Bellizzi D, Reali V, Fini M et al. 2012. Sirt3 protects from hypoxia and staurosporine-mediated cell death by maintaining mitochondrial membrane potential and intracellular ph. Cell Death and Differentiation. 19(11):1815-1825.

Pi H, Xu S, Reiter RJ, Guo P, Zhang L, Li Y, Li M, Cao Z, Tian L, Xie J et al. 2015. Sirt3-sod2-mros-dependent autophagy in cadmium-induced hepatotoxicity and salvage by melatonin. Autophagy. 11(7):1037-1051.

Pillai VB, Sundaresan NR, Jeevanandam V, Gupta MP. 2010. Mitochondrial sirt3 and heart disease. Cardiovascular Research. 88(2):250-256.

Pratheeshkumar P, Son Y-O, Divya SP, Turcios L, Roy RV, Hitron JA, Wang L, Kim D, Dai J, Asha P et al. 2016. Hexavalent chromium induces malignant transformation of human lung bronchial epithelial cells via ros-dependent activation of mir-21-pdcd4 signaling. Oncotarget. 7(32):51193-51210.

Qiao A, Wang K, Yuan Y, Guan Y, Ren X, Li L, Chen X, Li F, Chen AF, Zhou J et al. 2016. Sirt3-mediated mitophagy protects tumor cells against apoptosis under hypoxia. Oncotarget. 7(28):43390-43400.

Riganti C, Gazzano E, Polimeni M, Aldieri E, Ghigo D. 2012. The pentose phosphate pathway: An antioxidant defense and a crossroad in tumor cell fate. Free Radical Biology & Medicine. 53(3):421-436.

Robey RB, Hay N. 2009. Is akt the "warburg kinase"?-akt-energy metabolism interactions and oncogenesis. Seminars In Cancer Biology. 19(1):25-31.

Ryan HE, Lo J, Johnson RS. 1998. Hif-1 alpha is required for solid tumor formation and embryonic vascularization. The EMBO Journal. 17(11):3005-3015.

Sano H, Eguez L, Teruel MN, Fukuda M, Chuang TD, Chavez JA, Lienhard GE, McGraw TE. 2007. Rab10, a target of the as160 rab gap, is required for insulin-stimulated translocation of glut4 to the adipocyte plasma membrane. Cell Metabolism. 5(4):293-303.

Sano H, Roach WG, Peck GR, Fukuda M, Lienhard GE. 2008. Rab10 in insulin-stimulated glut4 translocation. The Biochemical Journal. 411(1):89-95.

Sasaki H, Sato H, Kuriyama-Matsumura K, Sato K, Maebara K, Wang H, Tamba M, Itoh K, Yamamoto M, Bannai S. 2002. Electrophile response element-

mediated induction of the cystine/glutamate exchange transporter gene expression. The Journal of Biological Chemistry. 277(47):44765-44771.

Satterstrom FK, Swindell WR, Laurent G, Vyas S, Bulyk ML, Haigis MC. 2015. Nuclear respiratory factor 2 induces sirt3 expression. Aging Cell. 14(5):818-825.

Sekhar KR, Crooks PA, Sonar VN, Friedman DB, Chan JY, Meredith MJ, Starnes JH, Kelton KR, Summar SR, Sasi S et al. 2003. Nadph oxidase activity is essential for keap1/nrf2-mediated induction of gclc in response to 2-indol-3-yl-methylenequinuclidin-3-ols. Cancer Research. 63(17):5636-5645.

Semenza GL. 2010. Hif-1: Upstream and downstream of cancer metabolism. Current Opinion in Genetics & Development. 20(1):51-56.

Shackelford DB, Vasquez DS, Corbeil J, Wu S, Leblanc M, Wu CL, Vera DR, Shaw RJ. 2009. Mtor and hif-1alpha-mediated tumor metabolism in an lkb1 mouse model of peutz-jeghers syndrome. Proceedings of the National Academy of Sciences of the United States of America. 106(27):11137-11142.

Shallari S, Schwartz C, Hasko A, Morel JL. 1998. Heavy metals in soils and plants of serpentine and industrial sites of albania. The Science of the Total Environment. 209(2-3):133-142.

Shi XL, Dalal NS. 1989. Chromium (v) and hydroxyl radical formation during the glutathione reductase-catalyzed reduction of chromium (vi). Biochemical and Biophysical Research Communications. 163(1):627-634.

Shibata T, Ohta T, Tong KI, Kokubu A, Odogawa R, Tsuta K, Asamura H, Yamamoto M, Hirohashi S. 2008. Cancer related mutations in nrf2 impair its recognition by keap1-cul3 e3 ligase and promote malignancy. Proceedings of the National Academy of Sciences of the United States of America. 105(36):13568-13573.

Singh A, Boldin-Adamsky S, Thimmulappa RK, Rath SK, Ashush H, Coulter J, Blackford A, Goodman SN, Bunz F, Watson WH et al. 2008. Rnai-mediated silencing of nuclear factor erythroid-2-related factor 2 gene expression in non-small cell lung cancer inhibits tumor growth and increases efficacy of chemotherapy. Cancer Research. 68(19):7975-7984.

Solis LM, Behrens C, Dong W, Suraokar M, Ozburn NC, Moran CA, Corvalan AH, Biswal S, Swisher SG, Bekele BN et al. 2010. Nrf2 and keap1 abnormalities in non-small cell lung carcinoma and association with clinicopathologic features. Clinical Cancer Research : an Official Journal of the American Association for Cancer Research. 16(14):3743-3753.

Someya S, Yu W, Hallows WC, Xu J, Vann JM, Leeuwenburgh C, Tanokura M, Denu JM, Prolla TA. 2010. Sirt3 mediates reduction of oxidative damage and prevention of age-related hearing loss under caloric restriction. Cell. 143(5):802-812.

Son YO, Pratheeshkumar P, Roy RV, Hitron JA, Wang L, Zhang Z, Shi X. 2014. Nrf2/p62 signaling in apoptosis resistance and its role in cadmium-induced carcinogenesis. The Journal of biological chemistry. 289(41):28660-28675.

Sporn MB, Liby KT. 2012. Nrf2 and cancer: The good, the bad and the importance of context. Nature Reviews Cancer. 12(8):564-571.

Stasinos S, Zabetakis I. 2013. The uptake of nickel and chromium from irrigation water by potatoes, carrots and onions. Ecotoxicology and Environmental Safety. 91:122-128.

Stein SC, Woods A, Jones NA, Davison MD, Carling D. 2000. The regulation of amp-activated protein kinase by phosphorylation. The Biochemical Journal. 345 Pt 3:437-443.

Stohs SJ, Bagchi D, Hassoun E, Bagchi M. 2000. Oxidative mechanisms in the toxicity of chromium and cadmium ions. Journal of Environmental Pathology, Toxicology and Oncology : Official Organ of the International Society for Environmental Toxicology and Cancer. 19(3):201-213.

Sun H, Brocato J, Costa M. 2015. Oral chromium exposure and toxicity. Current Environmental Health Reports. 2(3):295-303.

Suzuki M, Otsuki A, Keleku-Lukwete N, Yamamoto M. 2016. Overview of redox regulation by keap1–nrf2 system in toxicology and cancer. Current Opinion in Toxicology. 1:29-36.

Tchounwou PB, Yedjou CG, Patlolla AK, Sutton DJ. 2012. Heavy metals toxicity and the environment. EXS. 101:133-164.

Tong KI, Katoh Y, Kusunoki H, Itoh K, Tanaka T, Yamamoto M. 2006. Keap1 recruits neh2 through binding to etge and dlg motifs: Characterization of the two-site molecular recognition model. Molecular and Cellular Biology. 26(8):2887-2900.

United States. Occupational S, Health A. 2009. Hexavalent chromium. Washington, D.C.]: Washington, D.C. : U.S. Dept. of Labor, Occupational Safety and Health Administration.

Vaupel P. 2004. The role of hypoxia-induced factors in tumor progression. The Oncologist. 9 Suppl 5:10-17.

Wang X, Son YO, Chang Q, Sun L, Hitron JA, Budhraja A, Zhang Z, Ke Z, Chen F, Luo J et al. 2011. Nadph oxidase activation is required in reactive oxygen species generation and cell transformation induced by hexavalent chromium. Toxicological Sciences : an Official Journal of the Society of Toxicology. 123(2):399-410.

Wang XJ, Sun Z, Villeneuve NF, Zhang S, Zhao F, Li Y, Chen W, Yi X, Zheng W, Wondrak GT et al. 2008. Nrf2 enhances resistance of cancer cells to chemotherapeutic drugs, the dark side of nrf2. Carcinogenesis. 29(6):1235-1243.

Wang Y-Y, Chen J, Liu X-M, Zhao R, Zhe H. 2018. Nrf2-mediated metabolic reprogramming in cancer. Oxidative Medicine and Cellular Longevity. 2018:9304091.

Warburg O. 1956a. On respiratory impairment in cancer cells. Science (New York, NY). 124(3215):269-270.

Warburg O. 1956b. On the origin of cancer cells. Science (New York, NY). 123(3191):309-314.

Ward PS, Thompson CB. 2012. Metabolic reprogramming: A cancer hallmark even warburg did not anticipate. Cancer Cell. 21(3):297-308.

Wei H, Liu L, Chen Q. 2015. Selective removal of mitochondria via mitophagy: Distinct pathways for different mitochondrial stresses. Biochimica Et Biophysica Acta. 1853(10 Pt B):2784-2790.

Welling R, Beaumont JJ, Petersen SJ, Alexeeff GV, Steinmaus C. 2015. Chromium vi and stomach cancer: A meta-analysis of the current epidemiological evidence. Occupational and Environmental Medicine. 72(2):151-159.

Wende AR, Young ME, Chatham J, Zhang J, Rajasekaran NS, Darley-Usmar VM. 2016. Redox biology and the interface between bioenergetics, autophagy and circadian control of metabolism. Free Radical Biology & Medicine. 100:94-107.

Wilbur S, Abadin H, Fay M, Yu D, Tencza B, Ingerman L, Klotzbach J, James S. 2012. Agency for toxic substances and disease registry (atsdr) toxicological profiles. Toxicological profile for chromium. Atlanta (GA): Agency for Toxic Substances and Disease Registry (US).

Woodruff TJ, Axelrad DA, Caldwell J, Morello-Frosch R, Rosenbaum A. 1998. Public health implications of 1990 air toxics concentrations across the united states. Environmental Health Perspectives. 106(5):245-251.

Yang W, Nagasawa K, Munch C, Xu Y, Satterstrom K, Jeong S, Hayes SD, Jedrychowski MP, Vyas FS, Zaganjor E et al. 2016. Mitochondrial sirtuin network reveals dynamic sirt3-dependent deacetylation in response to membrane depolarization. Cell. 167(4):985-1000.e1021.

Yao H, Guo L, Jiang BH, Luo J, Shi X. 2008. Oxidative stress and chromium(vi) carcinogenesis. Journal of environmental pathology, toxicology and oncology : official organ of the International Society for Environmental Toxicology and Cancer. 27(2):77-88.

Ye J, Zhang X, Young HA, Mao Y, Shi X. 1995. Chromium(vi)-induced nuclear factor-kappa b activation in intact cells via free radical reactions. Carcinogenesis. 16(10):2401-2405.

Yu W, Gao B, Li N, Wang J, Qiu C, Zhang G, Liu M, Zhang R, Li C, Ji G et al. 2016. Sirt3 deficiency exacerbates diabetic cardiac dysfunction: Role of foxo3a-parkin-mediated mitophagy. Biochimica Et Biophysica Acta.

Zhang H, Davies KJA, Forman HJ. 2015a. Oxidative stress response and nrf2 signaling in aging. Free Radical Biology & Medicine. 88(Pt B):314-336.

Zhang J, Wang J, Xing H, Li Q, Zhao Q, Li J. 2016a. Down-regulation of fbp1 by zeb1-mediated repression confers to growth and invasion in lung cancer cells. Molecular and Cellular Biochemistry. 411(1-2):331-340.

Zhang JY, Deng YN, Zhang M, Su H, Qu QM. 2016b. Sirt3 acts as a neuroprotective agent in rotenone-induced parkinson cell model. Neurochemical Research. 41(7):1761-1773.

Zhang P, Singh A, Yegnasubramanian S, Esopi D, Kombairaju P, Bodas M, Wu H, Bova SG, Biswal S. 2010. Loss of kelch-like ech-associated protein 1 function in prostate cancer cells causes chemoresistance and radioresistance and promotes tumor growth. Molecular Cancer Therapeutics. 9(2):336-346.

Zhang Z, Pratheeshkumar P, Budhraja A, Son YO, Kim D, Shi X. 2015b. Role of reactive oxygen species in arsenic-induced transformation of human lung bronchial epithelial (beas-2b) cells. Biochemical and Biophysical Research Communications. 456(2):643-648.

Zhitkovich A. 2005. Importance of chromium-DNA adducts in mutagenicity and toxicity of chromium(vi). Chemical Research in Toxicology. 18(1):3-11.

Zhitkovich A. 2011. Chromium in drinking water: Sources, metabolism, and cancer risks. Chemical Research in Toxicology. 24(10):1617-1629.

Zhong H, De Marzo AM, Laughner E, Lim M, Hilton DA, Zagzag D, Buechler P, Isaacs WB, Semenza GL, Simons JW. 1999. Overexpression of hypoxia-inducible factor 1alpha in common human cancers and their metastases. Cancer Research. 59(22):5830-5835.

Zou D, Liu P, Chen K, Xie Q, Liang X, Bai Q, Zhou Q, Liu K, Zhang T, Zhu J et al. 2015. Correction: Protective effects of myricetin on acute hypoxia-induced exercise intolerance and mitochondrial impairments in rats. Plos One. 10(7):e0133336.

VITA

Name: Marco Antonio de Freitas Clementino

1. Education

06/2014   B.S. Baccalaureate in Biological Sciences, Universidade Federal do Ceara

07/2012 - 07/2013   Science without Borders Study Abroad Program, The University of Western Australia, Australia

2. Professional positions held

01/2009 – 07/2009   Undergraduate Researcher at Laboratory of the Vegetal Biotechnology laboratory, Department of Biochemistry and Molecular Biology, Universidade Federal do Ceará, Brazil

07/2010 – 02/2011   Undergraduate Researcher at Laboratory of Vegetal Biotechnology, Department of Biochemistry and Molecular Biology, Universidade Federal do Ceará, Brazil

03/2011 – 12/2011   Biochemistry class tutor at the Department of Biochemistry and Molecular Biology, Universidade Federal do Ceará, Brazil

01/2012 – 06/2012   Undergraduate Researcher at the Laboratory of Pharmacology, Poisons and Toxins, Biomedical Institute of the Brazilian Semi Arid, Universidade Federal do Ceará, Brazil

08/2013 – 06/2014   Undergraduate Researcher at the Laboratory of Molecular Toxicology, Biomedical Institute of the Brazilian Semi Arid, Universidade Federal do Ceará, Brazil.

01/2015 – 03/2019   Research Assistant at the Department of Toxicology and Cancer Biology, University of Kentucky

3. Professional publications

Havt, A; Lima, IFN; Medeiros, PHQS; **Clementino, M;** *et al.* Prevalence and virulence gene profiling of enteroaggregative *Escherichia coli* in malnourished and nourished Brazilian children. Diagnostic Microbiology and Infectious Disease, 89(2):98-105, 2017

Clementino M, Shi X, Zhang Z. Prevention of polyphenols against carcinogenesis induced by environmental carcinogens. *Journal of Experimental Toxicology, Oncology, and Pathology.* 36:87-98, 2017

Clementino M, Shi X, Zhang Z. Metabolic reprogramming and metal carcinogenesis. *Current Opinion in Toxicology.* 8:20-27, 2018

Prata, MMG; Cavalcante, PA; Silva, AVA; Medeiros, PHQS; Reyes, MAV; Quetz, JS; **Clementino, MAF;** *et al.* Alanyl-Glutamine protects against damage by enteroaggregative *Escherichia coli* strains in intestinal cells. Accepted for publication. September 2018. *Journal of Pediatric Gastroenterology and Nutrition.*

Howard, N; **Clementino, M**; *et al.* New developments in mechanisms of prostate cancer progression. Accepted for publication. September 2018. *Seminars in Cancer Biology.*

Clementino M, Kim D, and Zhang Z. Constitutive Activation of NAD-Dependent Sirtuin 3 plays an Important Role in Tumorigenesis of Chromium(VI)-Transformed cells. Accepted for publication. January 2019. Toxicological Sciences.

Clementino M, Kim D, Zhang Z. Nrf2 Constitutive Activation Induces Metabolic Shift, Leading to Increased Tumorigenesis Of Chromium(VI)-Transformed Cells. In writing.